Multifunctional Conjugates for Fluorescence and Magnetic Resonance Imaging

Thesis by
Brian P. Johnson

In Partial Fulfillment of the Requirements for the Degree of
Master of Science

California Institute of Technology
Pasadena, California

Submitted August 20, 2001

Acknowledgements

Most of all, I would like to thank my parents, sister, other family members and friends for their love and support throughout my studies.

Thanks to Tom Meade for accepting me into his group and for opening my eyes to the biological side of coordination chemistry. Thanks in particular for the timely motivational jumpstarts and general enthusiasm.

To the Meade group, Matt Allen, Joe Duimstra, Joe Fassler, Frank Femia, Angie Louie, Jeremiah Miller, Rex Moats, and Carlo Quiñonez, thanks for all helpful advice and, to those of you who actually brought doughnuts to group meeting, thanks for the doughnuts. In particular, thanks to Matt and Frank for the congenial work atmosphere and for the much-needed afternoon snack trips.

Thanks to Scott Fraser for his encouragement and for making Fraserland a positive and exciting place to do research. To the members of Fraserland, thanks for having patience with a chemist's first introduction to certain bio-thingamabobs. Namely, thanks to Andy Ewald for carrying out some fluorescence experiments and to Mike Tyszka for some MRI experiments. Thanks also to Meghan, Mag, Mary D, Ivan, Andy, Ying, Jason, Reinhard, Carole, Helen, Jim, Cyrus, and Robia for making work an especially friendly place to be.

Special thanks to Dian Buchness, Mary Flowers, Kathleen Hand, and Diana St. James for invaluable assistance and especially for all pleasant chat sessions and spirited bantering.

Thanks also to Matt, Frank, and Angie for proofreading and advice concerning this manuscript.

Table of Contents

Abstract

Computer-enhanced light microscopy imaging and magnetic resonance imaging (MRI) have emerged as leading techniques for *in vivo* monitoring of intact organisms. Employing the advantages of both techniques, a set of bifunctional, polymeric imaging agents is presented. A high-molecular weight, membrane impermeable scaffold such as dextran was chosen, so that the imaging agent would be trapped inside cells after injection. The molecular framework is covalently functionalized with multiple units of both gadolinium-diethylenetriaminepentaacetic acid and a fluorescent dye, such as 1,1'-dioctadecyl-3,3,3',3'-tetramethylindocarbocyanine (DiI). The synthesis of this class of reporter probes is versatile, allowing for varying wavelengths of attached fluorophores and types of MRI agents to be used.

1 Introduction

The investigation of cell lineage and patterning of the central nervous system is an active area of research.[1-3] Such studies are crucial to the understanding of adult vertebrate development and involve the tracing of individual cells or tissues, including their progeny, any rearrangements, migrations, interactions, and even cell death.[2] Direct observation of this complex intermingling of events is further complicated by the opacity of the developing embryo and the sheer number of optically indistinguishable cells involved.[4-9]

The study of the movements and fates of cells in intact, living embryos has been revolutionized by the emergence of computer-enhanced light microscopy and magnetic resonance imaging (MRI) as the two predominant imaging techniques currently used in research and clinical applications, respectively.[9-11] Both techniques use contrast agents, which are molecular entities that enhance the signals of the images obtained. In light microscopy, photoluminescent compounds called fluorophores are injected into the specimens and viewed with a fluorescence microscope. For MRI, chelated paramagnetic metal centers are injected and subsequently increase the measured signal of neighboring water molecules, thus creating contrast from bulk water.

Throughout the development of both optical and magnetic imaging techniques, there has been great impetus for the development of contrast agents that go beyond just their detection within living systems. Contrast agents are continually being synthesized to express a known property or serve a specific function within that system,[12-14] and these functions include specific organelle binding, detection of enzymatic activity, responses to pH and temperature, and many more. Though the agents used for fluorescence

microscopy and MRI are generally chemically different (organic fluorophores vs. metal centers), specific agents can be covalently linked to form conjugates useful for either application. As a result, two disparate imaging methods are combined at the molecular level in the synthesis of a single compound that enhances both optical and magnetic signals.

2 Background

2.1 Fluorescence Microscopy Basics

Fluorescence microscopy is one of the most ubiquitous imaging techniques used in developmental biology. Fluorescence is a physical property by which light is absorbed by molecules at a particular wavelength and subsequently emitted at a longer wavelength. The difference in excitation and emission wavelengths, the Stokes shift, is dependent upon the fluorescent molecules under study and with the aid of single-wavelength excitation sources and optical filters, offers a certain degree of chemical selectivity in microscopy experiments.

Several naturally occurring substances such as NADH, riboflavin, and flavin coenzymes fluoresce at a detectable level, particularly at wavelengths below 300 nm, and the virtual omnipresence of these species gives rise to a baseline optical signal in nearly all biological specimens. With some exceptions,[15] this autofluorescence is often discarded as background noise. In order to create optical contrast between structures of interest and background autofluorescence, fluorescent probes are injected into samples. These probes consist of natural fluorescent dyes, such as green fluorescent protein and related substances extracted from deep-sea jellyfish among other sources, but are often synthetic fluorophores, which can be constructed to fit specific optical attributes. The

most desirable fluorophores exhibit high photostability, high extinction coefficients, high quantum yields, and a large Stokes shift.[16] There is also a vast field of synthetic fluorescent dyes demonstrating antibody receptor targeting,[17] organelle affinity, and chemical sensing.[18]

In general, fluorescence microscopy is highly sensitive, needing as few as fifty fluorescent molecules per cubic micrometer for detection in cellular studies.[16] The method is also able to reach subcellular resolution, with the actual resolution limit depending on the objective lens and aperture of the microscope employed.[19-21] However, the major limitation involved is the depth at which samples can be imaged. Most modern optical techniques can view only the top hundred or so microns, due to optical aberrations coupled with absorption and scattering of light by tissue.[22] To circumvent this problem, many experiments are limited to exterior features and events, and when interior information is of interest, specimens are subject to histological procedures at different embryonic stages and sectioned to allow imaging of deep structures. In that scenario, some of the observations are derived from inference and are therefore contaminated by manipulation artifacts.

Optical microscopy techniques remain the most widely used imaging methods in biological laboratories. However, in order to observe cellular phenomena within embryos that have developed beyond the transparent stages, high-resolution magnetic resonance imaging has emerged as a powerful technique.

2.2 MRI Basics

Magnetic resonance imaging was developed during the 1970s as the result of the discovery of nuclear magnetic resonance (NMR) thirty years earlier and has since become a leading diagnostic device as well as an important method for imaging large-scale biological specimens.[23] MRI makes use of the most abundant molecule in biological tissues, water. When subjected to a magnetic field, the spin vectors of the protons of water molecules orient themselves along the magnetic field vector. When a radio-frequency pulse is then applied to the system, the proton spin vectors are randomized and reorient themselves to the original magnetic field vector over a measurable amount of time. This process of realignment is called relaxation, and it is the signal resulting from the measured relaxation times, T_1 (spin-lattice) and T_2 (spin-spin), that gives rise to any MR image.

Water protons in different tissues will relax at inherently different rates, rendering various tissues distinguishable from one another. However, greater detail and experimental versatility are achieved by the addition of MRI contrast agents, which are materials that modify neighboring water proton relaxation rates and thus enhance the local signal. Certain agents, referred to as T_1-weighted agents, feature a paramagnetic metal center that interacts directly (inner-sphere) and remotely (outer-sphere) with water protons and dramatically accelerates their T_1 relaxation rates.

In theory, any paramagnetic metal can be used as an MRI contrast agent, but in practice, the most widely used is the lanthanide ion, Gd^{3+}, whose seven unpaired electrons give it the highest magnetic moment ($\mu^2 = 63BM^2$) of any mononuclear species[24] and a symmetric electronic ground state (S^8). However, the Gd^{3+} aqua ion is

extremely toxic and must be chelated to a strongly binding ligand to reduce toxicity. It is this chelation restraint, though, that makes the chemistry of contrast agents so rich. Gd^{3+} typically has nine coordination sites, and when fewer than nine coordination sites are bound by a chelate, at least one site remains free to interact with water molecules. Hence, the foremost challenge in developing MRI contrast agents is the design of chelates that bind Gd^{3+} strongly enough to render the ion nontoxic and yet allow enough interaction with water to generate a strong MRI signal.

At the present time, scores of MRI contrast agents exist and have been thoroughly reviewed elsewhere.[23,25] Some of the more common contrast agents are shown in Figure 1. Each of these three agents makes use of an octadentate ligand with hard donating carboxy and amine groups, which bind especially well to the Gd^{3+} ion. The ninth remaining site binds weakly with the oxygen-donor of water molecules, and this site is in rapid exchange with water molecules from the bulk solution.

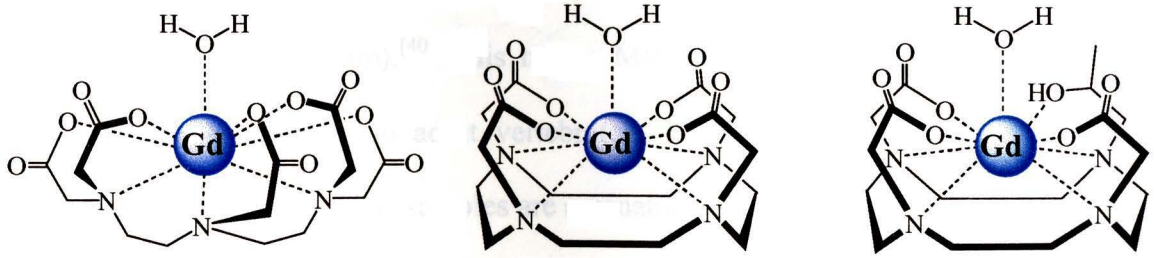

$[Gd(DTPA)(H_2O)]^{2-}$ Magnevist™ | $[Gd(DOTA)(H_2O)]^{-}$ Dotarem™ | $[Gd(HP\text{-}DO3A)(H_2O)]$ ProHance™

Figure 1. Common MRI contrast agents.

There is currently a major experimental thrust towards the development of novel, more elaborate MRI contrast agents. Within the past decade, contrast agents have been synthesized, which sense changes in temperature[26-28] and pH,[29-35] detect Ca^{2+} ions,[36]

and report on enzymatic activity and gene expression,[11,37] among other functions,[14] including targeting and sensory applications.[38,39]

Such extensive interest in contrast agents derives from the usefulness of MRI as a technique. Since only the water proton spin relaxation rates are measured, MRI is completely non-invasive, as long as the contrast agent can be safely excreted. The non-invasive nature of MRI differs from fluorescence microscopy, in which toxic effects result from phototoxic byproducts released by photobleaching of some of the fluorescent dyes. MRI is also a truly three-dimensional (3D) imaging technique; three field gradients are set orthogonally, and the resulting image comes from a matrix of intensities representing individual volume elements (voxels). 3D images are indeed obtainable by fluorescence microscopy as well, but require a longer time scale, due to the necessary sectioning and staining procedures, and are subject to the imaging artifacts outlined above.

Compared to light microscopy, resolution in MRI is low, but is still able to reach the cellular level (ca. 10μm).[40] This makes MRI ideally suited for larger specimens, from developing embryos to adult vertebrates. Since MRI does not rely on optical inspection, completely opaque samples are amenable.

The combination of fluorescence and MR techniques creates a powerful imaging arsenal. Specifically for developing embryos, fluorescence microscopy allows for the precise observation of cell labeling at the earliest embryological stages, while MRI can be applied for long-term monitoring of cell lineage and interaction throughout the later stages. In the case where a singular bifunctional agent is employed, the power of both techniques can be exploited to monitor the local environment of one molecule in a single

biological specimen, thus simplifying the system and allowing for its thorough investigation.

2.3 Bifunctional Agents

The development of bifunctional agents for twofold imaging purposes is not a new idea. Multiple units of fluorescent dyes and MRI contrast agents have been tethered to biomolecules,[41-43] and single-unit monomeric examples have recently become

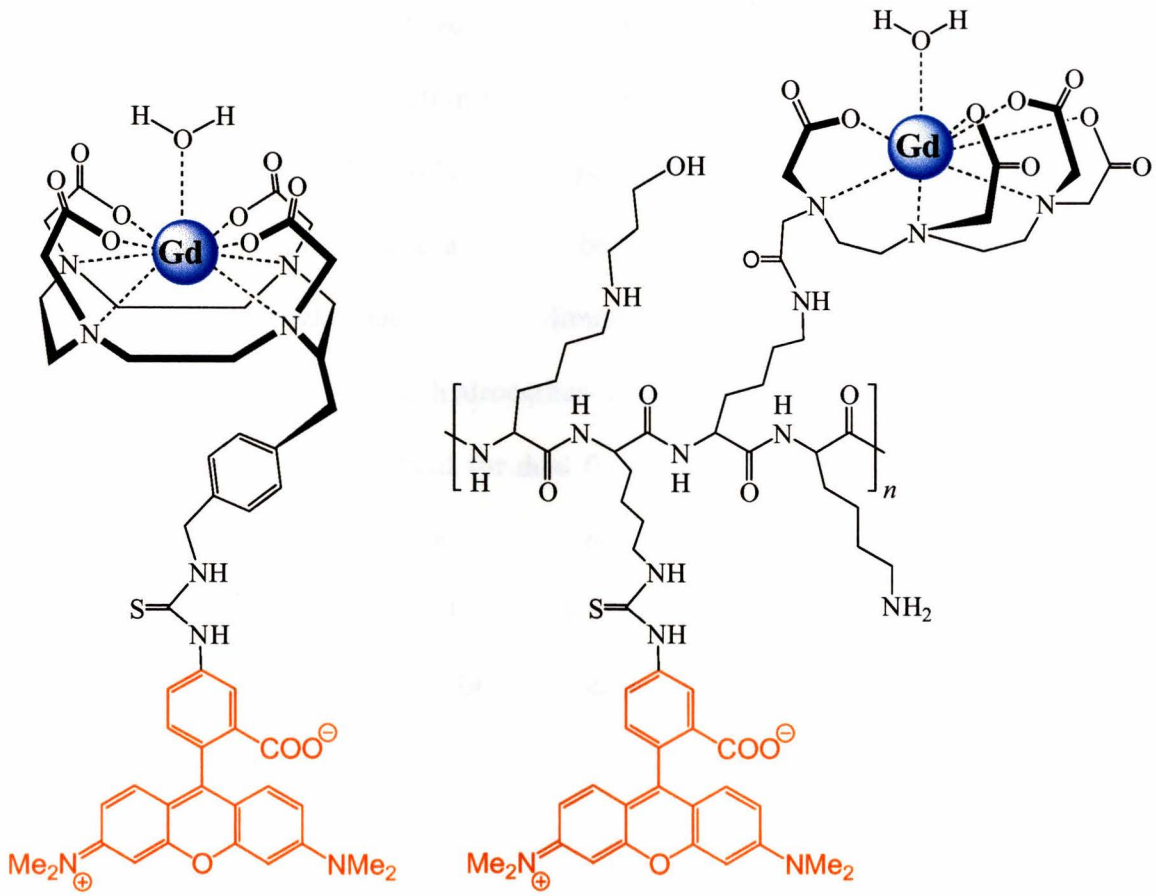

Gd(rhoda-DOTA) GRIP

Figure 2. Two examples of bifunctional fluorescence and MRI contrast agents: Gd(rhoda-DOTA) and GRIP.

accessible due to the increasing availability of metal chelates bearing amine-reactive functional groups.[43-51] One recent agent taking advantage of such dual-purpose chelates is the monomeric Gd(rhoda-DOTA) (Figure 2) which is characterized by one Gd-DOTA complex covalently attached to one unit of the fluorescent dye tetramethylrhodamine by a *p*-thiourea-benzyl linker.[42] This agent was proposed as a tool for investigating membrane permeability and fusion, gap-junctional communication, and lesions.

Fluorescence microscopy is particularly sensitive; therefore, an agent bearing only one fluorescent dye is sufficient for most purposes. MRI is less sensitive, and since MRI studies are often long-term and are carried out in larger specimens, MRI contrast agents are subject to considerable dilution inside the system being analyzed. As a result, it is advantageous for MRI agents to bear multiple units of the paramagnetic metal.[52] Many molecular scaffolds are suitable and have been used for multiple MRI contrast agent labeling. These include but are not limited to polypeptides,[42] dendrimers,[53,54] polysaccharides,[42] and simple hydrocarbon polymers.[55] One polypeptide system, in particular, offers an ideal scaffold for dual fluorophore/MR contrast agent conjugation. With its already available reactive amines, poly-D-lysine has been functionalized with multiple units of Gd-DTPA chelates and tetramethylrhodamine dyes.[42] This agent, known as GRIP (Figure 2), is membrane impermeable and therefore suited to cell lineage studies.

2.4 Dextran and MION Particles

Along with Gd(rhoda-DOTA) and GRIP, the Hüber paper described a bifunctional contrast agent built onto a dextran backbone. This polysaccharide system has

the advantage of being extremely water-soluble and completely inert unlike GRIP, whose abundant amines had to be protected in order to curb toxicity. In the original article,[42] a dextran conjugate analogous to GRIP was synthesized with multiple units of Gd-DTPA complexes and tetramethylrhodamine. It was thought that the dextran scaffold represented an exceptionally versatile system for synthesizing a wider array of multifunctional conjugates involving different fluorophores and types of MR contrast agent.

Another less developed system envisioned as a versatile support for multifunctional imaging agents is the microcrystalline iron oxide nanoparticle (MION). This nanometer-sized particle is composed of paramagnetic iron oxide clusters, which accelerate the T_2 relaxation rates of nearby water protons, and are additionally coated with reactive amines amenable to conjugation with other imaging agents. This system is convenient in that it already has the MR contrast agent built in, and with MION particles, the less studied area of T_2-weighted imaging agents can be further explored.

In previous work with the dextran system, some synthetic details were ambiguous or missing, and some of the conjugates were not well characterized at the molecular level. Herein is described a more thorough synthetic approach and optimization for an MRI active dextran template and its conjugates involving a range of fluorescent dyes. Also discussed are the beginnings of synthetic conjugates, which use MION particles as foundations for conjugating fluorescent dyes and other bioactive molecules.

3 Synthesis of Conjugates

3.1 Dextran Conjugates

Dextran is a membrane-impermeable polysaccharide of glucose monomers connected by 1,6 α-glycosidic linkages and can vary in molecular weight from about 3000 to 40+ million daltons. Dextran chains of moderate size (less than a hundred thousand daltons) are exceptionally water soluble, making dextran a suitable scaffold for contrast agent labeling. Many fluorescent dyes and some MRI contrast agents do not dissolve well in aqueous systems. A large number of these agents can essentially be "dragged" into solution by the covalent bonds that attach them to the water-soluble dextran backbone.

The most conventional route for single labeling of dextran involves monofunctionalization at the reducing terminus of the chain. Every dextran chain contains exactly one aldehyde group at the terminus, even when branching exists.[56] By reductive amination, the aldehyde can be reacted either with a diamine to yield a singly labeled dextran-amine or directly with the free amines of peptides or other biomolecules. This approach is especially useful in cancer treatment when the terminus is labeled with a targeting agent that recognizes cancer-cell membrane receptors, while the rest of the dextran is covalently decorated with multiple units of a drug or radionuclide.[57]

For fluorescence and MR imaging purposes, a higher load of imaging labels is needed. Unlike poly-D-lysine, the monomers of dextran have no obvious functional groups for attaching multiple contrast agents and must therefore be modified with reactive linkers, and several synthetic routes for this have been established.[58-61] For example, reaction of dextran with periodate results in the oxidation of multiple glucose

alcohols to aldehydes, thus creating the more reactive polyaldehyde dextran. As with the terminus aldehyde chemistry described above, reductive amination subsequently offers two modes of conjugation.

3.1.1 Dextran Amination

Since many fluorophores and chelates for MRI agents are available in several amine reactive forms, a multiply aminated dextran is most desirable in the present study. Although the polyaldehyde dextran route is often employed, polyamino dextran is isolated more directly from a one-pot synthesis via activation with cyanogen bromide (BrCN) and subsequent reaction with a diamine. In basic aqueous solution, BrCN deprotonates slightly acidic alcohols to form a cyanooxy group, which is hydrolyzed to a primary carbamate *in situ*, which then reacts with primary amines to form a secondary carbamate (Scheme 1).

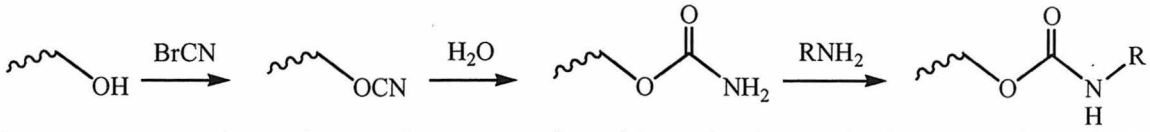

Scheme 1. Reaction scheme of cyanogen bromide activation and subsequent hydrolysis and carbamate formation.

The reaction sequence in Scheme 1 is versatile in that a wide array of molecules can be attached to the parent alcohol. In the case of the dextran scaffold, multiple units of R can be attached, and any side products can be washed away easily by purification of the resulting dextran conjugate. This attribute has been exploited in a host of applications where biomolecules of interest have been conjugated directly to dextran by cyanogen

bromide activation. Enzymes have been conjugated for immobilization for the purpose of added stability and preservation of enzymatic activity.[62-64] Multiple covalent linking of dextran has been used in the delivery of certain tumor targeting agents,[65] enzyme inhibitors,[66] and drugs[67-69] for prolonged pharmaceutical activity and better control of the drugs' properties.

When RNH_2 in Scheme 1 is a diamine, one amine is used for the carbamate formation, while the other amine remains available for further conjugation to another agent. In the reaction with dextran, BrCN activation takes place selectively at the alcohol of the 5-carbon position, since that is the only position β to three other electron-withdrawing oxygen atoms and therefore creates the most acidic alcohol. Subsequent hydrolysis and reaction with 1,6-diaminohexane leads to the multiply aminated dextran, DexAm (**1**) (Scheme 2).

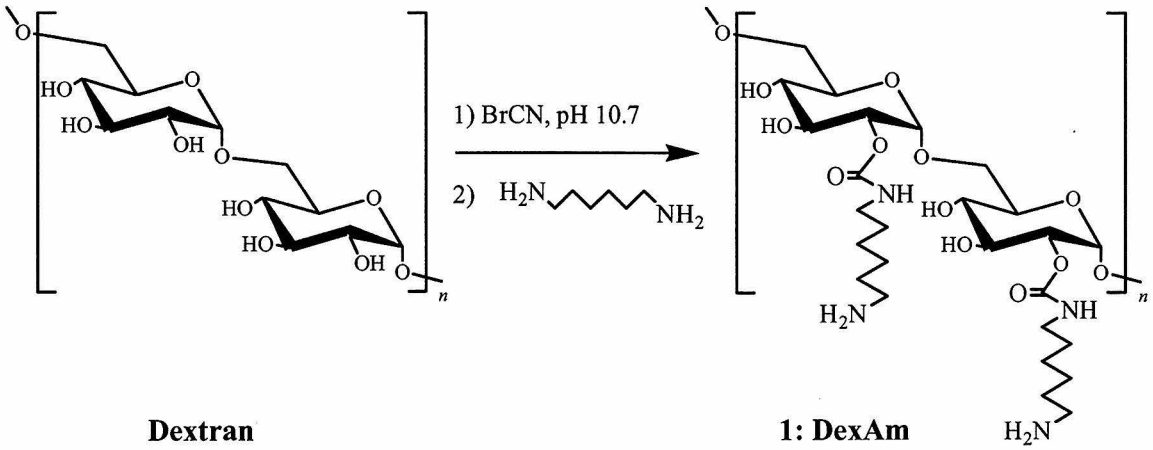

Scheme 2. Amination of dextran by BrCN activation and reaction with 1,6-diaminohexane.

Throughout this study, a dextran chain of average molecular weight 10,500 was used, which corresponds to a 65-monomer chain length. For the purpose of conjugating

imaging agents to this chain, any alkyl or aryl diamine can be used for the reaction in Scheme 2, and ethylene diamine has been employed previously.[70] Use of the longer and extremely flexible 6-carbon alkyl diamine offers the advantage that the resulting conjugates bear imaging agents spaced farther from the dextran backbone, and this would presumably alleviate any potential disruption of the contrast agents' properties by the relatively massive polysaccharide.

In this study, conditions for carrying out the amination step in Scheme 2 were taken from a literature method designed in the Meade group by Hüber *et al.*[42] This protocol had been adapted from a previously reported synthesis using the same basic reagents,[71] but the Hüber preparation was slightly ambiguous and lacking in some experimental details. For example, the final DexAm polymer was purified by FPLC using a phosphate buffer as the eluent, but no details of removal of the phosphate and counter ions from the product are supplied. In a first attempt to follow this preparation, the DexAm product was isolated with phosphate buffer impurities, and removal of these ions was attempted by a combination of gel chromatography techniques including a C18 reverse-phase column. In each case, phosphate ions were detected in the final product by ^{31}P NMR spectroscopy. Several attempts to purify DexAm by FPLC without the use of phosphate buffers were carried out. Using a buffer-free eluent, i.e. pure water, gave poor separation. Several volatile buffers were also probed as possible eluents, such as ammonium carbonate and ammonium acetate, but these eluents tended to give inconsistent chromatograms that rarely contained peaks of isolable product. As a result, the method of FPLC was abandoned, and purification by dialysis was inspected.

Dialysis offers the advantage that it can be set up and basically ignored for several days while carrying out other tasks, as opposed to FPLC, which required literally hundreds of injections for the purification of any sample amounting to more than a gram. The crude reaction mixture was simply loaded into dialysis bags of molecular weight cut-off (MWCO) 3500 and placed in a bath of stirring water, and the water was changed every morning and evening, until it was determined by monitoring the supernatant water by UV-vis spectroscopy that no further dialysis was required (until no UV signal was detectable against a deionized water blank). In the preparation in Scheme 2, the only mononuclear ions used in the synthesis of DexAm were Na^+, Cl^-, and Br^-, and none of these three elements was detectable in the dialysis purified product by elemental analysis. This led to the conclusion that dialysis was a suitable purification method for DexAm, and dialysis would then be used in later steps.

In producing the DexAm polymer, all reactive amine groups for later conjugation are provided in a single step. As a result, all subsequent steps are limited by the yield of amines resulting from this first step. For this reason, it was deemed appropriate to invest time into quantifying the number of free amines available on each dextran chain of DexAm, which had not been measured in the Hüber preparation. This quantification would ultimately lead to a means of optimizing the yield of free amines.

Methods for detecting and quantifying primary amino groups are readily available in the literature.[72-75] Two prevalent spectroscopic methodologies are by use of the ninhydrin[76-78] and fluorescamine[79,80] reagents, which represent absorption and fluorescent techniques, respectively. As shown in Scheme 3, free amines react with ninhydrin to form Ruhemann's purple, which absorbs intensely at 570 nm, while

ninhydrin itself absorbs negligibly at 570 nm. However, reactions with ninhydrin require heating to temperatures of 100°C or greaters and, in experiments with DexAm, did not consistently run to completion, thus thwarting quantification. With fluorescamine, primary amines react at room temperature within a few hundred milliseconds to form a fluorescent compound (Scheme 3) while fluorescamine itself is not fluorescent.

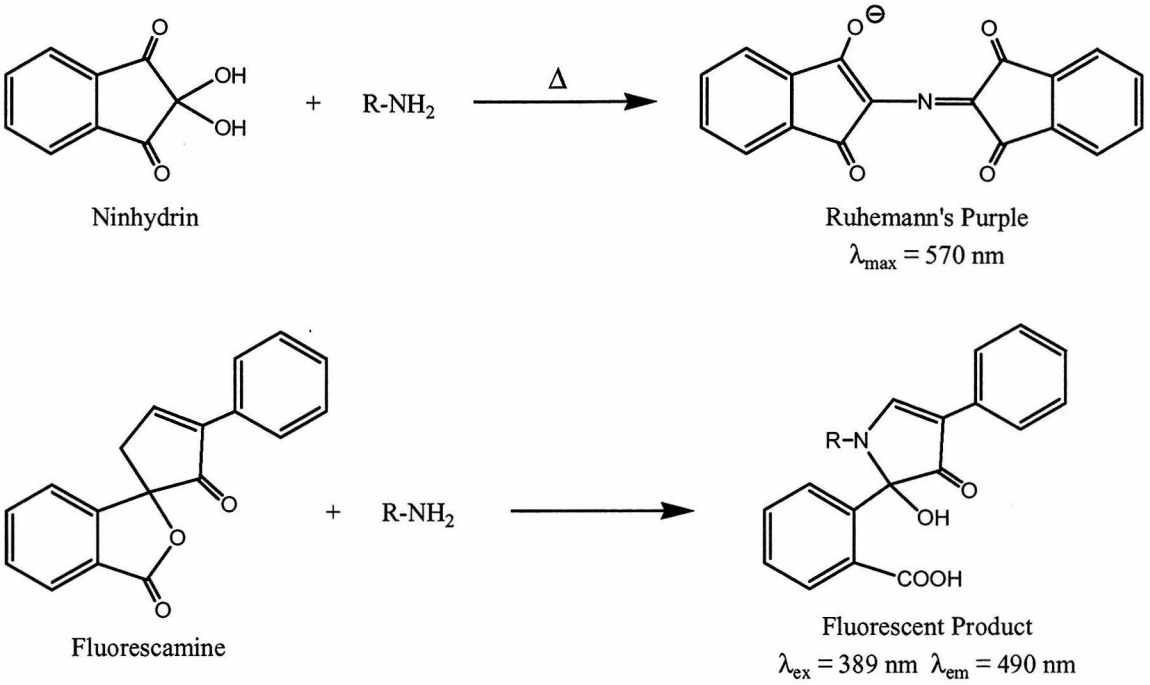

Scheme 3. Reaction of ninhydrin and fluorescamine with primary amines to form spectroscopically quantifiable products.

Experiments to probe this technique resulted in the observation that, at least in the DexAm matrix, the fluorophore generated is subject to self-quenching pathways and leads to erratic measurements. This was evidenced by plots of emission versus concentration that were linear only within a range but were not one-to-one outside that range. The data from within the linear range did not agree with the amine quantification

using elemental analysis (results shown later), and the method of using fluorescamine was abandoned in favor of more reliable methods.

Other attempts to quantify the number of free amines on the DexAm polymer included titration of an aqueous solution of DexAm with a standardized solution of HCl. The resulting pH curve inflection points were too numerous and not sharp enough to derive conclusive values for the number of free amines. The inflection points that were present did indicate that for the 65mer glucose polymer used, somewhere between 5 and 30 free amines were present. Though this was not a concrete quantification, it was evidence that the anticipated load of 10 to 20 amines per 65mer chain was a reasonable estimation.

As one final effort to quantify the free amines in DexAm, elemental analysis was employed as a tool that does not rely on the solution behavior of the amines present. As a preliminary trial, elemental analysis was carried out on every element that had come into contact with DexAm during the synthesis and purification, i.e. C, H, N, O, Na, Cl, and Br. In each sample measured, no Na, Cl, or Br was found above the detection threshold. As a result, it was logically presumed that the only matter in the purified sample was aminated dextran. In order to quantify the number of aminations on the dextran chain, it is simpler to view the sample as a mixture of two components, glucose and the 6-aminohexylcarbamate entity conjugated to the glucose during amination (Scheme 4). Addition of the sums of the individual masses of the two components gives the total mass of the sample. In Scheme 4, DexAm is broken into its individual glucose (Glu) and 6-aminohexylcarbamate (Am) components, which contribute molecular weights of 162 and 144, respectively. By considering a sample of total mass, z, and defining variables for the

total moles of Glu and Am, x and y respectively, then simple algebra allows us to find the ratio of aminated glucose to total glucose monomers present, y/x. By these definitions, x represents all glucose monomers, whether aminated or not. The number of aminations, y, in a given sample of mass z is determined by spectroscopy. In the case where elemental data is used, z is given an arbitrary mass (e.g. 1 g), and y is calculated as z times (%N/14)/2. Division by two is necessary because each aminated monomer contributes two nitrogen atoms, and both N atoms are measured in elemental analysis. Multiplication of the ratio y/x by 65 gives an estimate for the number of aminations per 65mer dextran on a sample of DexAm. As mentioned above, the expression derived in Scheme 4 can be applied to data collected from either elemental analysis or spectroscopic measurements.

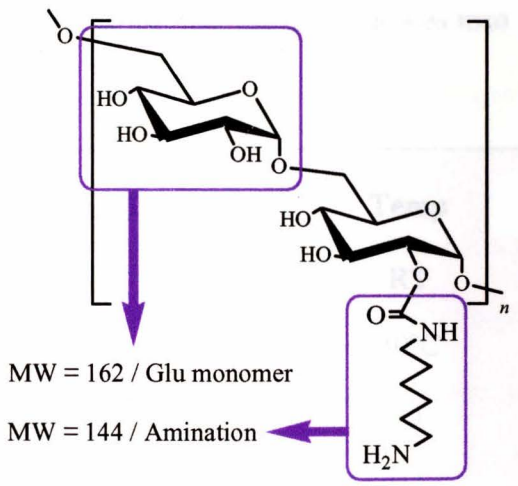

Let x = total moles of Glucose monomers in sample
Let y = moles of aminated monomers in sample
Let z = total mass of sample

(x moles Glu)(162 g/mol) = 162x
(y moles Am)(144 g/mol) = 144y
162x + 144y = z

x = (z-144y)/162

y/x = fraction of Glu monomers aminated
65(y/x) = number of aminations per 65mer dextran

Scheme 4. Mathematical derivation of the number of aminations per 65mer dextran. This expression can be utilized for elemental analysis data and/or spectroscopic data.

Given a means for amine quantification, the synthesis of DexAm was ready for optimization. In the Hüber preparation,[42] the experimental description is ambiguous in that the stoichiometric relationship of the BrCN to dextran is unclear. As a way of

simplifying and thus better communicating the experimental conditions, the synthesis of DexAm should be presented in terms of the number of monomers of glucose employed rather than the amount of dextran. In those terms, the number of equivalents BrCN reacted per equivalent glucose in previous Meade group protocol was 0.38. It was hypothesized that increasing the BrCN concentration per glucose equivalent would enhance the final load of primary amines on DexAm. Because other variables may influence the efficiency of the reaction, it was decided to vary the equivalents of BrCN per Glu monomer, temperature, and concentration of the dextran in aqueous solution. Shown in Table 1 are some of the combinations of conditions surveyed. Increasing the equivalents of BrCN and/or temperature led to immediate crosslinking of the dextran chain, as evidenced by the reactants precipitating out of solution and creating a white to off-white tar-like material that was insoluble even in boiling DMSO (189°C).

Entry	Equiv. BrCN	Temp	Vol. H_2O / g Dex	Result
1*	0.38	RT	200 mL	unoptimized yield of $-NH_2$
1a	1.20	40°C	200 mL	extensive crosslinking
1b	2.50	RT	200 mL	immediate crosslinking
1c	1.20	RT	200 mL	extensive crosslinking
1d	0.90	RT	200 mL	crosslinking evident
1e	0.67	RT	200 mL	crosslinking evident
1f	0.67	RT	400 mL	no observed crosslinking

Table 1. Optimization of dextran amination. * - Entry 1 represents the conditions used in the literature preparation[42] and previous laboratory protocol, both of which served as starting conditions for optimizing.

Even at slightly less than one equivalent BrCN per Glu (Entry 1d), crosslinking was evident. So, by lessening the amount of BrCN to 0.67 equivalents per Glu and by lowering the concentration of dextran in solution to 400 mL H_2O per g dextran, a suitable product was obtained. Although more combinations of conditions were available, the resulting product in Entry 1f would suffice for further synthetic steps. In comparison to the conditions previously used (Entry 1*), the product from Entry 1f showed a greater abundance of nitrogen by elemental analysis, 2.68% in Entry 1f versus 1.75% in Entry 1*. By using the equation in Scheme 4, these translate to 12 versus 7 primary amines, respectively, per 65mer dextran. For Entry 1f, the amount of dextran used was 2.30g. Attempts to scale up this reaction to the 8 g level were successful but not very practical because of the large volumes of water that had to be evaporated for purification (on this scale, approximately 3400 mL water must be evaporated, which takes about 20 hours, and this is unavoidable because the crude DexAm reaction solution must be concentrated before dialysis).

There are no published reports of NMR spectra for DexAm. In earlier usage of DexAm for conjugation of imaging agents, the final conjugates were characterized based on their imaging properties, and synthetic intermediates were not characterized thoroughly. However, the role of DexAm as a limiting factor in dictating the maximum number of agents to be conjugated makes the first step the most important.

The ^1H NMR spectrum of DexAm in D_2O shows a cluster of multiplets between 3.3 and 3.8 ppm and a slightly broadened doublet at 4.95 ppm, which correspond to the glucose monomer ring protons. In addition, broad peaks appear at 1.33, 1.55, 2.86, 3.04, and 3.14 ppm, which show the amino alkyl protons, with the latter two peaks shifted

downfield from the parent 1,6-diaminohexane due to the electron-withdrawing carbamate functionality. In the ^{13}C NMR spectrum, six peaks between 67 and 99 ppm represent the six glucose monomer carbons, while six peaks are found upfield and are identifiable as the amino alkyl carbons. A small cluster of peaks is observed between 155 and 165 ppm, which is typical for ^{13}C carbamate resonances.[81] This verifies that the amino alkyl groups are attached covalently to the dextran chain. The carbamate linker is further evidenced by the IR spectrum of DexAm, in which absorbances appear at 1713 and 1230 cm^{-1}, typical for carbamate groups.[81] Although the spectroscopic data confirms the presence of product, 1,6-diaminohexane may exist as an impurity, which would not be detected by elemental analysis or spectroscopy. To check for the presence of free 1,6-diaminohexane (MW = 117), an electrospray mass spectrum was taken of DexAm and did not reveal a peak for 1,6-diaminohexane, while a positive control consisting of DexAm spiked with 1,6-diaminohexane did show a peak at m/z = 117.2. With elemental, spectroscopic, and mass data, it was then concluded that DexAm was a pure product.

3.1.2 DTPA Addition

Subsequent to the amination step, DexAm was covalently modified with multiple units of an MRI contrast agent by reaction with a suitable Gd^{3+} chelate. The well-known diethylenetriaminepentaacetic acid (DTPA) chelate was chosen for this system for the following reasons: the conjugation of Gd-DTPA complexes to polysaccharide chains has been described,[71] and reaction of the commercially available DTPA dianhydride with primary amines readily affords the amido-DTPA derivative. This reaction in the dextran conjugation sequence is shown in Scheme 5.

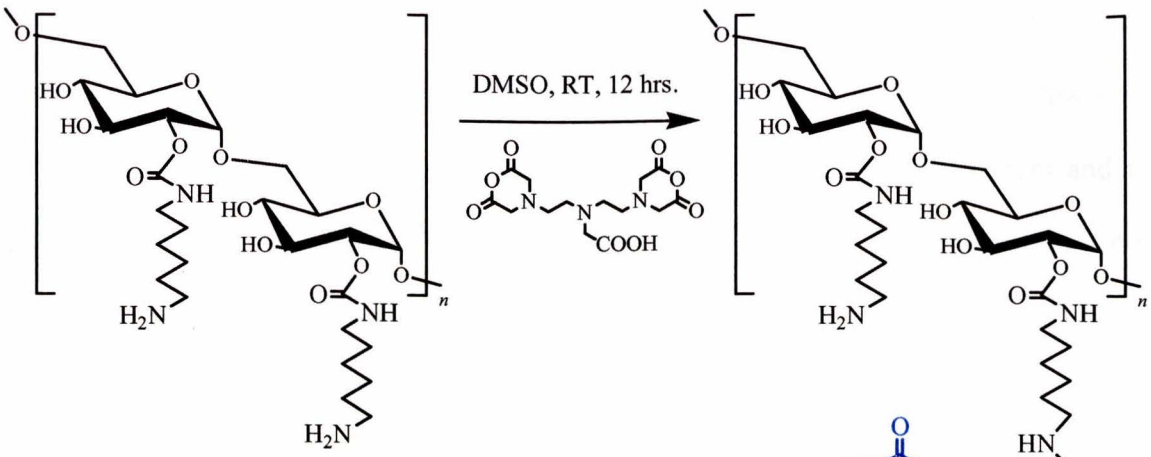

1: DexAm

2: DexAmDTPA (DAD)

Scheme 5. Reaction of DTPA dianhydride with DexAm.

Nucleophilic attack of the primary amines of DexAm on the electron deficient carbonyl groups of the cyclic anhydride functional groups leads to the amide linkage. This yields the DTPA chelate both covalently bound to the mother dextran chain and in tetracarboxylate form, which is suitable for Gd^{3+} chelation. This reaction must run in anhydrous conditions as each anhydride functional group is susceptible to the same nucleophilic attack by water. The reaction is run under large excess of DTPA dianhydride in order to reduce the number of crosslinked dextran chains. Once the reaction is finished, the entire mixture is quenched with water in order to open up the other cyclic anhydride.

The DTPA addition does not run in 100% yield. Herein lies the key to bifunctionality of dextran systems conjugated to imaging agents. It was desired that the final dextran conjugates be loaded with as much of the MRI contrast agent as possible

since larger loads of MRI agents are needed than for fluorescence. The aim in this study was to conjugate DTPA to all but a few amines on aminated dextran, leaving a few sites open for attachment to a fluorophore. As shown for the poly-D-lysine system and in previous studies in this lab with the dextran system, 100% yield of DTPA addition is not possible. Hence all DexAm templates in this study are loaded with as much DTPA as possible, since any large excess of DTPA dianhydride still leaves a few reactive amines for fluorophore attachment. At the end of each reaction, a quick *quali*tative test (which does work, as opposed to the *quanti*tative analyses) with ninhydrin or fluorescamine reveals the presence of primary amino groups, which confirms that subsequent fluorophore conjugation would still be accessible.

The purification of DexAmDTPA (or DAD) can be carried out in a number of ways. One problem that arose was the elimination of DMSO, which was not volatile enough to remove on the rotary evaporators or vacuum lines available. Dialysis was employed as a means of washing out the DMSO in exchange for pure water. Crude DMSO solutions were loaded into the dialysis bags to one-third or less capacity in order to allow for the influx of water; otherwise the bags would burst. Although dialysis proved sufficient for purification of DAD, it was time-consuming, and the DAD was exposed to copious amounts of water, which was undesirable since any aqueous metal impurities, Zn^{2+} in particular, coordinate to the DTPA chelates and inhibit Gd^{3+} metallation. This water exchange of DMSO through dialysis was questionable since the pore sizes of dialysis membranes are often affected adversely by large proportions of non-aqueous solvents. After all experiments in this study were completed, it was speculated that some

form of aqueous extraction with CH_2Cl_2 or Et_2O might be a more efficient technique and should be examined in future studies.

Characterization of DAD was not considered to be as imperative as with DexAm since Gd^{3+} metallation in the next step would quickly show how much of the MRI contrast agent had been conjugated. As with the Hüber paper, elemental analysis (C, H, N, O) served as an easy tool to measure the load of nitrogen. In most samples of DAD synthesized in this study, elemental analysis revealed that the quantity of nitrogen exceeded that of the theoretical case of 100% load of DTPA. This indicated that some DTPA (unconjugated) still remained in the sample as an impurity. It was decided that metallation with an excess of Gd^{3+} and subsequent purification would rid the sample of DTPA and any Gd-DTPA formed, and the next product could then be characterized based on its Gd content and aqueous relaxation properties.

3.1.3 Gd^{3+} Metallation

Once the free DTPA ligand is conjugated to the dextran chain, Gd^{3+} metallation is straightforward. Reaction of DAD with $GdCl_3$ in H_2O eliminates HCl, and by maintaining the pH at neutral or slightly basic levels and heating to 80°C, the reaction was presumably complete after 24 hours. This complexation with DAD is shown in Scheme 6.

The synthesis of Gd-DAD represents a vital stage in that, as previously mentioned, the load of MR contrast agent is of extreme importance for an operational bifunctional agent for long-term imaging. The characterization of Gd-DAD was carried out mainly via elemental analysis (C, H, N, O, Gd) and relaxivity data. The utility of

elemental data hinges on the ability to extract a measurement of the load of Gd-DTPA complexes per 65mer dextran.

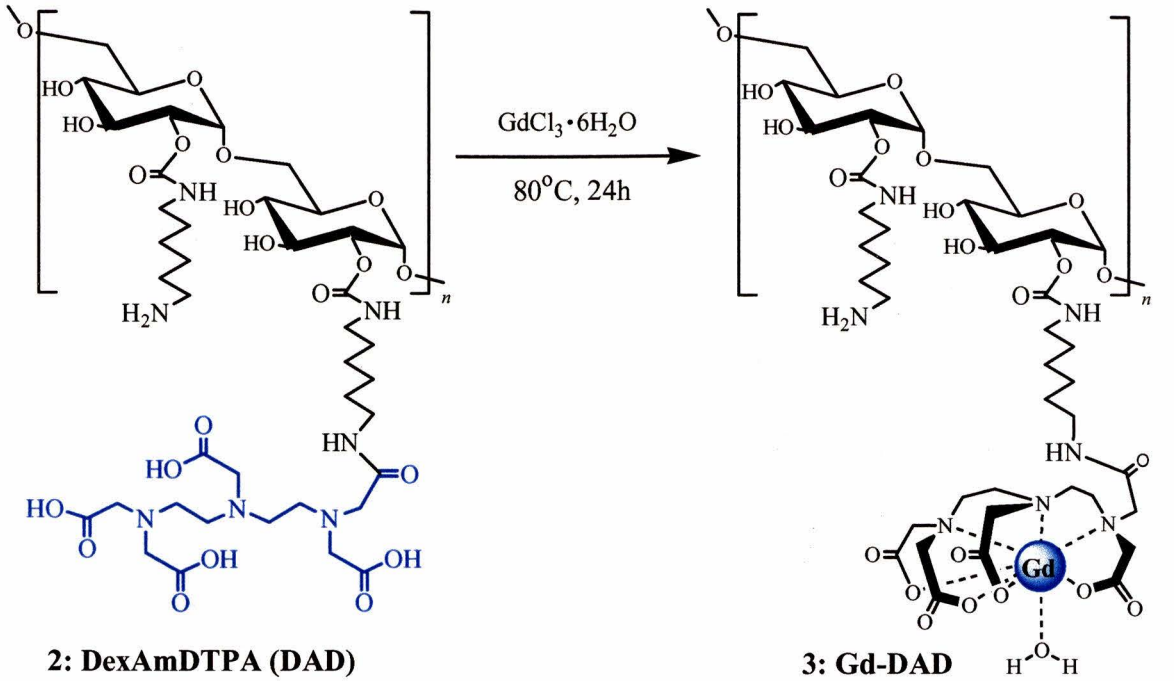

2: DexAmDTPA (DAD) **3: Gd-DAD**

Scheme 6. Metallation of DAD with Gd^{3+}.

In the following description is a mathematical derivation for the ratio of Gd-DTPA complexes (w) to the number of glucose monomers (z) on the parent dextran chain. The situation in Gd-DAD is much more complex than with DexAm (Scheme 4), in which only two species were present in the sample. In pure Gd-DAD, there are theoretically four monomer species present, which will be referred to as Glu, GluAm, GluAmDTPA (GAD), and Gd-GAD, and these are shown in Scheme 7.

The presence of GAD is included in recognition that Gd^{3+} metallation reactions do not always go in 100% yield, and this approach is more comprehensive than excluding the GAD species. The derivation for the ratio w/z is then based on the number of element

atoms each monomer species supplies in the sample. The only elements considered here are C, N, O, and Gd. Although H analysis is readily accessible, the amount of hydrogen is unreliable because several protonateable/deprotonateable functional groups are present

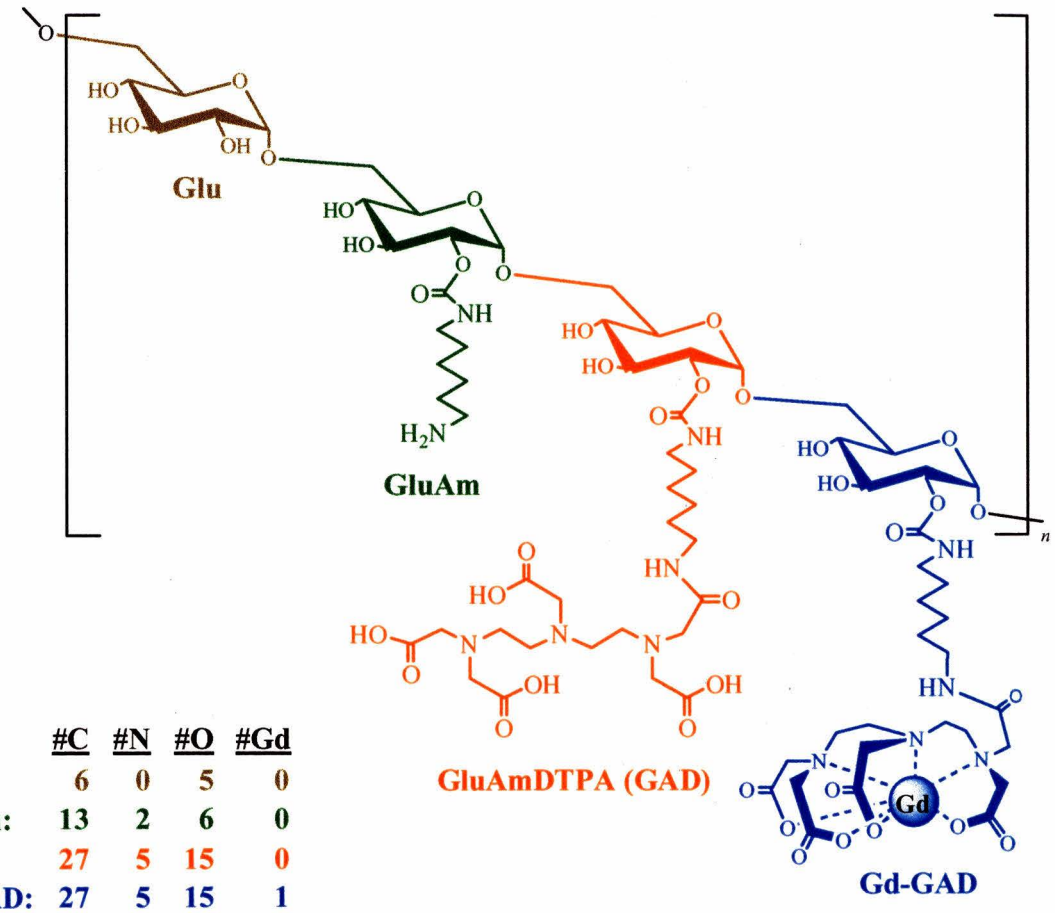

	#C	#N	#O	#Gd
Glu:	6	0	5	0
GluAm:	13	2	6	0
GAD:	27	5	15	0
Gd-GAD:	27	5	15	1

Let z = #(Glu + GluAm + GAD + Gd-GAD)
Let y = #(GluAm + GAD + Gd-GAD)
Let x = #(GAD + Gd-GAD)
Let w = #Gd-GAD

Then, z-y = #Glu
y-x = #GluAm
x-w = #GAD
w = #Gd-GAD

Scheme 7. Mathematical set-up of variables based on the number of element atoms each monomer type contributes.

that could shift the hydrogen content as a result of pH and wetness of the sample. Also, in contrast to DexAm, the Gd-DAD sample is more likely to contain salt impurities since

the conjugated Gd-DTPA complex is monoanionic and may be balanced by either protons or by alkali metals, such as the Na^+ used for pH adjustment during the reaction. Dialysis would presumably eliminate any alkali ions, but whether this is true or not becomes inconsequential because of the manner of elemental data manipulation. With this system, the absolute element percentages are not considered, but rather their relative ratios. As is shown below in the completed mathematical workup, elemental molar ratios from experimental data are used, and these correspond to the measured elemental percentage ratios. As such, any impurity that does not contain C, N, O, or Gd will not affect the outcome of the ratio w/z. It is assumed that free Gd-DTPA and free Gd^{3+} have been washed out by dialysis; clearance of Gd-DTPA and Gd^{3+} was confirmed by T_1 measurements of the supernatant bath. If these species were present in significant quantity, the ratio w/z would not accurately reflect the composition of Gd-DAD.

The total number of element atoms present in the sample can be expressed in terms of the variables in Scheme 7. By multiplying by the appropriate elemental molecular weight (12 for C, 14 for N, etc.), the number of moles of each element is expressed.

#C = 6z +7y +14x	molC = 72z + 84y + 168x	(1)
#N = 2y + 3x	molN = 28y + 42x	(2)
#O = 5z + y + 9x	molO = 80z + 16y + 144x	(3)
#Gd = w	molGd = 157.3w	(4)

Equations 1 - 4. Quantity of each element in terms of variables w, x, y, z.

At this point, three new variables must be defined, a, b, and c, the values of which are obtainable directly from the elemental data. Even though a, b, and c are expressed in

mole ratios, they can be stated interchangeably as elemental analysis percentage ratios. In the rest of this derivation, the variables a, b, and c are treated as constants, since their values are from experimental data and will be known when using the derived expression for w/z.

Define: $a = \frac{\text{molGd}}{\text{molC}}$ (5) $b = \frac{\text{molGd}}{\text{molN}}$ (6) $c = \frac{\text{molGd}}{\text{molO}}$ (7)

Then, $a = \frac{157.3w}{72z + 84y + 168x}$ (8) $b = \frac{157.3w}{28y + 42x}$ (9) $c = \frac{157.3w}{80z + 16y + 144x}$ (10)

Rearranging,

$$157.3w - 168ax - 84ay - 72ax = 0 \quad (11)$$
$$157.3w - 42bx - 28by = 0 \quad (12)$$
$$157.3w - 144cx - 16cy - 80cz = 0 \quad (13)$$

Equations 5 - 13. Definitions of experimental values a,b,c.

Substitution then leads to a system of three equations in four unknowns. This system is best manipulated in matrix form.

$$\begin{bmatrix} 157.3 & -168a & -84a & -72a \\ 157.3 & -42b & -28b & \\ 157.3 & -144c & -16c & -80c \end{bmatrix} \begin{bmatrix} w \\ x \\ y \\ z \end{bmatrix} = \begin{bmatrix} 0 \\ 0 \\ 0 \end{bmatrix} \quad (14)$$

Equation 14. Matrix form of derived system of equations.

Since this system has more variables than equations, the only completely obtainable solution set is the trivial solution, that is, w = x = y = z = 0. The desired ratio

w/z is accessible through a sequence of elementary Gaussian elimination operations, which require a sequence of algebraic steps not shown here.

$$w/z = \frac{44abc}{157.3(bc - \frac{14}{5}ac - \frac{7}{20}ab)} \qquad (15)$$

Equation 15. Solution of w/z in terms of C,N,O,Gd elemental data.

A quick mathematical check of this solution can be carried out by considering the theoretical situation, in which only monomers of the Gd-GAD type exist in the sample (i.e. w = x = y = z). In that case, elemental ratios are calculated based on the Gd-GAD monomer. These would be calculated as follows: a = 157.3/(27·12) = 0.4855, b = 157.3/(5·14) = 2.247, and c = 157.3/(15·16) = 0.6554. Substitution of these values into Eq. 15 gives w/z = 1, which should be true for the case that w = x = y = z, and this helps justify the solution derived.

Though this approach from elemental data from C, N, O, and Gd will work, there is still the issue of the unreliability of measurements of oxygen content. Whenever alkali metals or even lanthanides are present, which is likely the case in all Gd-DAD samples produced, oxygen measurements can be skewed by the formation of metal oxides. In addition, samples of Gd-DAD or hygroscopic and can either be wet upon synthesis or can even become wet during measurement of elemental content, thus thwarting accurate oxygen determination. The value in working through the above exercise, though it may not be used in every case, is that it serves as the mathematically purest approach to Gd-DTPA quantification. Every batch of Gd-DAD is different, depending on the researcher

who synthesized it, and it is important to quantify based on the most thorough approach (the above exercise) and compare with the simplified approach shown below. With both mathematical methods, the researcher producing Gd-DAD gets an idea of which method of quantification is more useful.

In order to manipulate elemental data that is absent of oxygen figures, only three monomer species can be considered; otherwise, too many equations will be present in the derived system. By assuming, however, that x is approximately equal to w, i.e. no GAD monomers exist and all DTPA chelates are complexed to Gd^{3+}, the situation presented in Scheme 8 results.

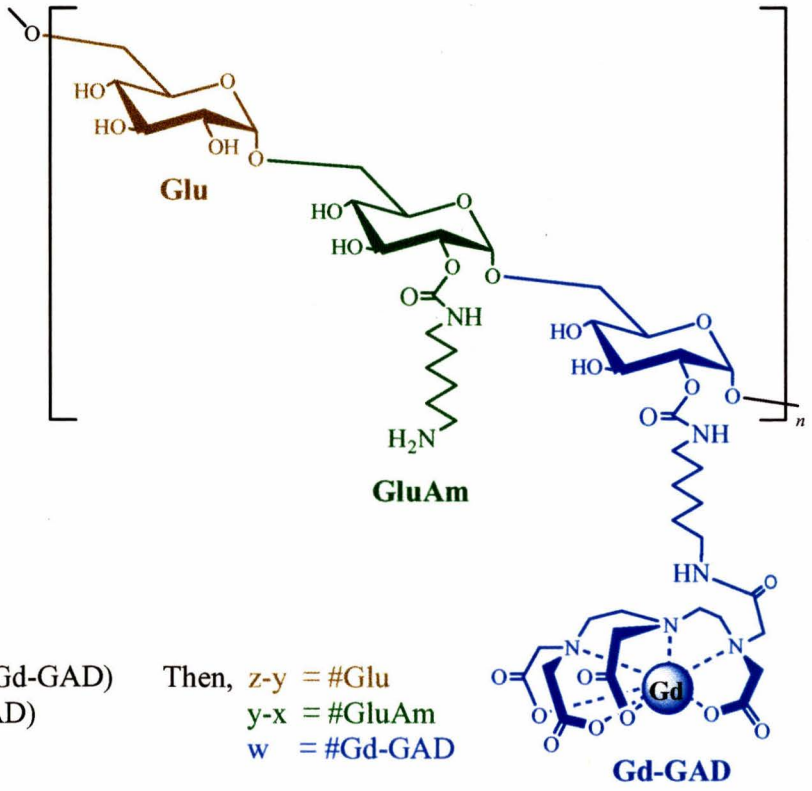

	#C	#N	#Gd
Glu:	6	0	0
GluAm:	13	2	0
Gd-GAD:	27	5	1

Let z = #(Glu + GluAm + Gd-GAD)
Let y = #(GluAm + Gd-GAD)
Let w = #Gd-GAD

Then, z-y = #Glu
y-x = #GluAm
w = #Gd-GAD

Scheme 8. Mathematical set-up of variables assuming no GAD present.

In this scenario, the mathematical treatment is the same as in the above case, and the algebra is much less involved. This results in the following solution for w/z. As with the previous solution, this simplified solution is easily checked by considering the theoretical case that all monomers are Gd-GAD.

$$w/z = \frac{72ab}{157.3b - 471.9a - 42ab} \qquad (16)$$

Equation 16. Solution of w/z in terms of C,N,Gd elemental data.

Regardless of the method of data analysis used, multiplication of the resulting w/z value by 65 gives the number of Gd-DTPA complexes on a typical 65mer dextran chain. For the samples of Gd-DAD synthesized in this study, between 5 and 10 Gd-DTPA complexes were found per 65mer. The principal Gd-DAD sample used in most of the subsequent fluorophore conjugation reactions had a load of 8 Gd-DTPA complexes (as calculated from the data presented for Gd-DAD in the Experimental Section). This value is lower than desired; however, this is a higher load, by 1 to 2 Gd-DTPA units, than the samples synthesized just before this study, as shown by elemental analyses of samples left over from previous researchers in this lab. For Gd-DAD samples in the current study, the result was the same to one significant figure, whether Eq. 15 or Eq. 16 was used. This indicates that, for simplicity sake, Eq. 16 should suffice for most purposes. It should be noted here that during the preparation of this manuscript, a comprehensive method for quantifying Gd-DTPA units on biomolecular scaffolds was reported.[82]

The goal of this work was to create a conjugate with a both a high load of Gd-DTPA and a relaxivity (based on moles Gd) comparable to free Gd-DTPA. To show that

Gd-DAD could function as an MRI contrast agent, T_1 data was gathered for several concentrations of Gd-DAD. Normally, a plot of $1/T_1$ versus molar concentration of the sample gives a linear trend, the slope of which is the relaxivity, r_1 (reported in units $mM^{-1}s^{-1}$), of the substance. In this case, molar concentration is essentially meaningless since Gd-DAD represents a conglomeration of molecules of different molecular weights; although the dextran used as starting material had a known average molecular weight, the product Gd-DAD has gone through a series of modifications and has an unknown molecular weight. For comparative magnitudes of relaxivity, Gd-DAD samples were measured in terms of grams rather than moles. Based on the elemental data of that same sample (i.e. by using the elemental data to convert mass quantities of Gd-DAD into molar quantities of Gd^{3+} in the sample), a measurement of relaxivity in $mM^{-1}s^{-1}$ could be calculated. For the Gd-DAD sample used in subsequent conjugations, the relaxivity was 5.82 $mM^{-1}s^{-1}$. This value is significantly higher than the relaxivity measured for Gd-DTPA by the Aime group (4.3 $mM^{-1}s^{-1}$)[83] and more recently by the Tweedle group (3.8 $mM^{-1}s^{-1}$)[84]. This increase in relaxivity of the Gd-DTPA complexes when conjugated to the dextran system is not surprising. One of the DTPA carboxylate groups is tied up in the amide bond to the hexyl carbamate group, thus weakening the donating ability at one position of the chelate, as amide carbonyls donate more weakly than carboxylate anions. This renders the Gd^{3+} center more exposed to the aqueous environment, thus creating more direct interaction with water molecules and accelerating their proton relaxation times. In addition, Gd^{3+} complexes tethered to biomacromolecules tend to display higher relaxivities as a result of the increase in rotational correlation time.[85] The overall result is an MRI agent with more power per Gd complex (higher r_1) but presumably with less

stability and potentially higher toxicity than unconjugated Gd-DTPA. Though other groups have used Gd-DTPA chelates tethered to other molecules by the same or similar chemistry,[55,82] only an *in vivo* study (shown later in this thesis) will show whether toxicity will be a concern for the particular case of Gd-DAD conjugates. With Gd-DAD synthesized, the dextran system can be reacted with a host of fluorophores to produce a series of bifunctional agents.

3.1.4 Bifunctional Dextran Agents

Many fluorophores are available with amine-reactive functional groups. Some of the more common functional groups that readily couple to amines include acid chlorides, carboxylic acids, sulfonyl chlorides, succinimidyl esters (SEs), and isothiocyanates (ITCs). In the case of acid chlorides, carboxylic acids, and SEs, extremely stable amide bonds are formed upon reaction with primary amines. With sulfonyl chlorides and ITCs, sulfonamides and thioureas are formed, respectively, and these are mostly stabile, with some decomposition occurring over time for the thiourea groups.[86] ITCs have been used for conjugation to the amine functionality of Gd-DAD in the Hüber preparation of GRID, a dextran agent bearing multiple Gd-DTPA complexes and tetramethylrhodamine units. This molecule was also synthesized in the current study, along with two other bifunctional agents that use the ITC group on the fluorophores fluorescein and pyrene. These syntheses are represented in Scheme 9.

Although many bifunctional conjugates are accessible via ITC derivatized fluorophores, reactions with ITC groups must be run in anhydrous conditions due to the sensitivity of the ITC group to hydrolysis. In order to run reactions in water and thus

open up more versatility in the fluorophore conjugation to Gd-DAD, fluorophores bearing succinimidyl ester groups were surveyed for their use in this step. These reactions are run in aqueous buffer adjusted to pH 8.0. A pair of conjugates made via the SE functionality is shown in Scheme 10.

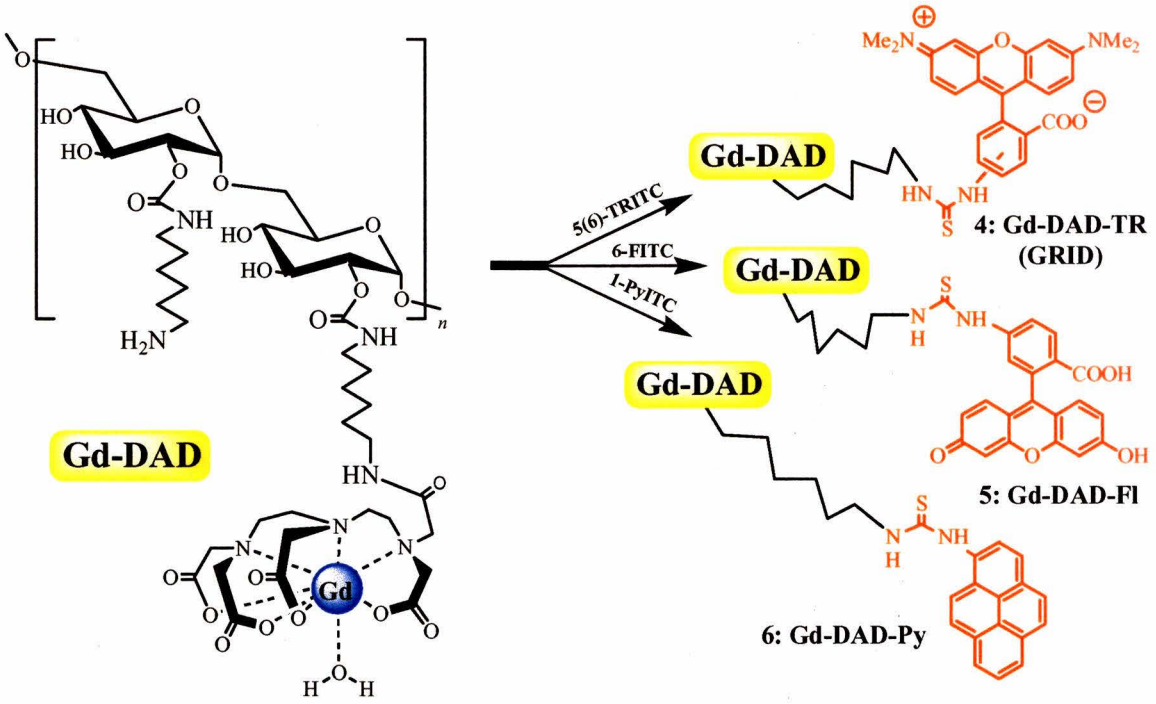

Scheme 9. Reaction of Gd-DAD with the amine-reactive fluorophores tetramethylrhodamine-5(6)-isothiocyanate (5(6)-TRITC), fluorescein-6-isothiocyanate (6-FITC), and pyrene-1-isothiocyanate (1-PyITC) to make compounds 4, 5, and 6, respectively.

Synthesizing a variety of bifunctional fluorescence and MRI agents begins to form an entire class of agents that offer a wide range of excitation/emission wavelengths. Nearly every fluorophore in current imaging use exists in some type of reactive form, the most common of which react with amine functionalities as described above. The goal in synthesizing the above agents is to show that the common amine reactive forms indeed work well with the Gd-DAD system.

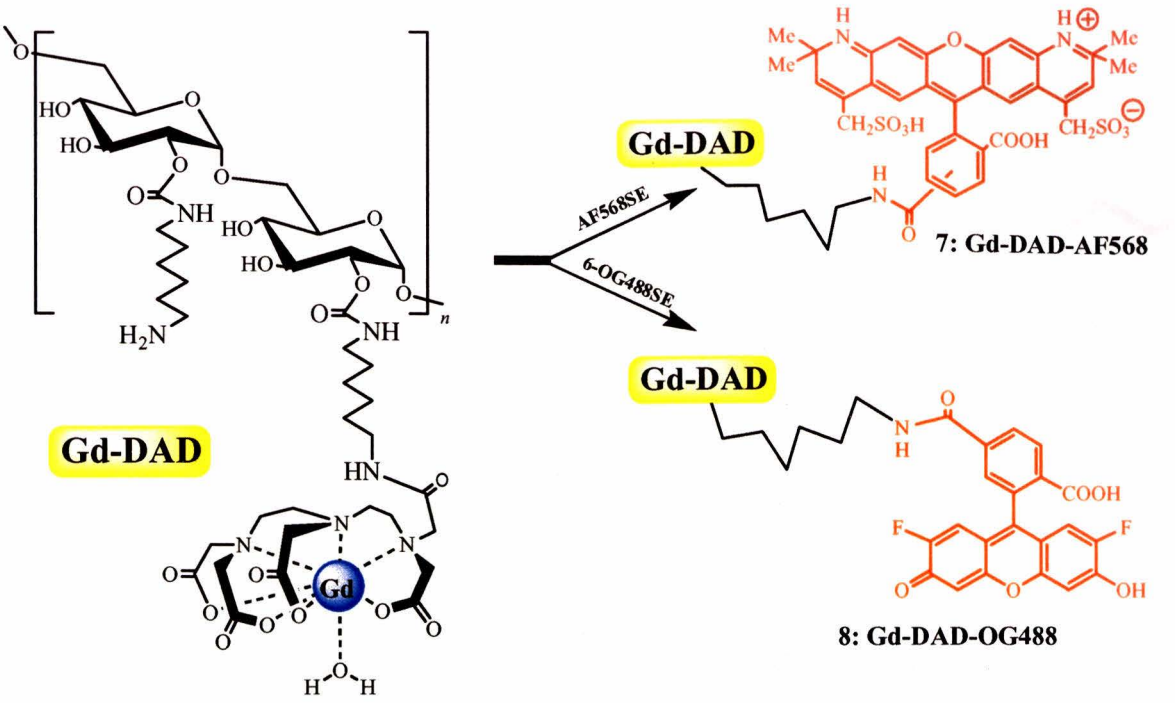

Scheme 10. Reaction of Gd-DAD with the amine-reactive fluorophores Alexa Fluor carboxylic acid, succinimidyl ester (AF568SE) and Oregon Green 488-6-carboxylic acid, succinimidyl ester (6-OG488SE) to make compounds 7 and 8, respectively.

In this study, the initial aspiration and motivation for making a series of bifunctional agents was the synthesis of a singular fluorescence/MRI agent that was simultaneously water-soluble and lipophilic. Such an agent would offer a means of monitoring cell lineages of the developing neural system extracellularly, as this agent would be envisioned to "stick" to the outsides of cell membranes and bring the imaging moieties along via the covalent linkers. The fluorescent probe 1,1'-dioctadecyl-3,3,3',3'-tetramethylindocarbocyanine (DiI), along with other carbocyanine dyes, has been used extensively in cell lineage studies.[86] The two 18-carbon alkyl chains make it extremely lipophilic, allowing the alkyl chains to infiltrate the cell membrane and pull the conjugated ring system along with it.[86]

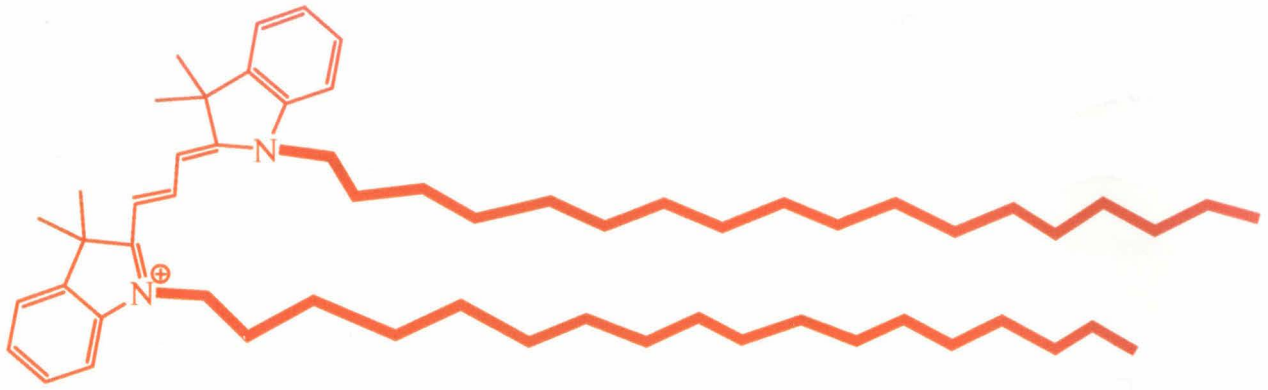

Figure 3. 1,1'-dioctadecyl-3,3,3',3'-tetramethylindocarbocyanine (DiI)

In routine applications of DiI in biological systems, this agent must be injected as an aqueous solution comprising about 20% ethanol, in order to achieve a suitable concentration, as DiI is not especially soluble in water. Dextran is highly water soluble, so the conjugation of DiI to the dextran template would then achieve water solubility and allow for injections without the use of ethanol (a high ethanol content is undesirable for injections since physiological fluids are essentially 100% aqueous). The utility of this proposed agent is convenient in that the lipophilic portion of the overall agent is inherent in the fluorophore itself, so no further synthetic steps are necessary to achieve this effect.

DiI is not commercially available in any typical amine reactive form, although the acid chloride and isothiocyanate exist in the patent literature.[87] Synthesis of the isothiocyanate form from a commercially available amine precursor would be possible, but the precursor is exceedingly expensive. Rather than take this route, it was found that the commercially available Cell Tracker™ form of DiI contained a (4-chloromethyl-benzoylamino)-methyl linker at the 5-position. Though this agent is not marketed as an amine-reactive form, the chlorobenzyl functionality has been shown as a useful linker to

groups containing secondary amines.[88] It was understood that primary amines would be more reactive to the chlorobenzyl group than secondary amines, and indeed, reaction of 5-[(4-chloromethyl-benzoylamino)-methyl]-DiI (CM-DiI) proceeded in DMSO at 80°C in the presence of K_2CO_3, as shown in Scheme 11.

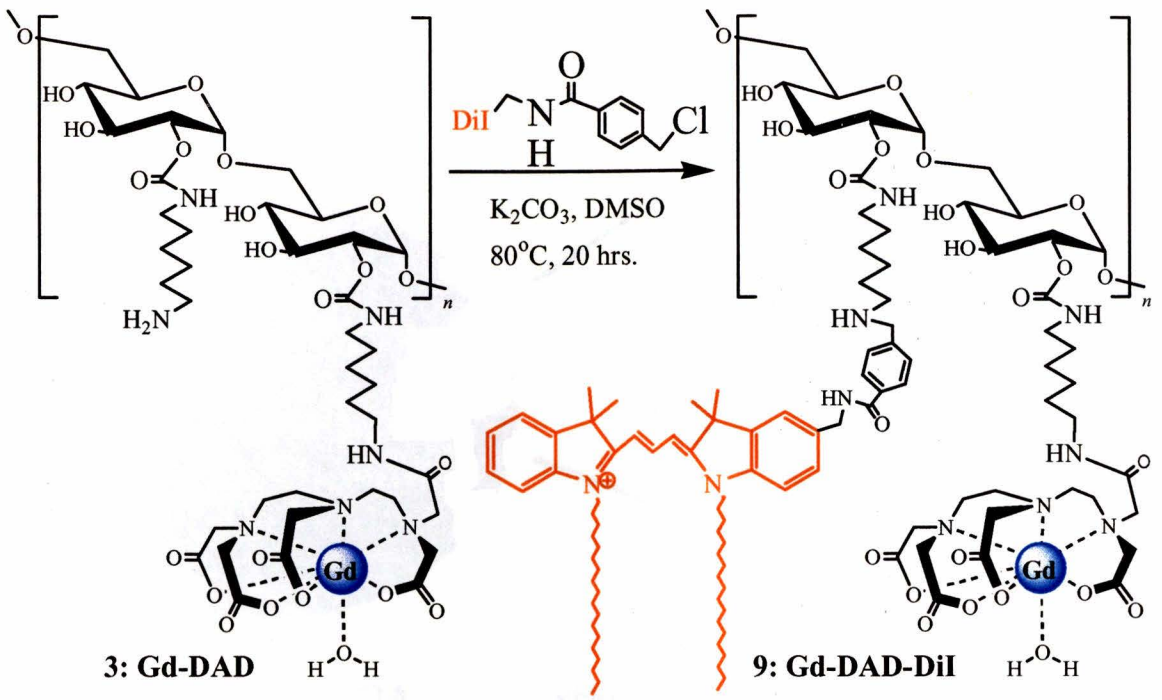

Scheme 11. Synthesis of Gd-DAD-DiI by use of chlorobenzyl functionality.

Using a KNO_3(sat.)/H_2O/CH_3CN (1:6:93) solution, the reaction was monitored by TLC until CM-DiI could no longer be detected. The synthesis of the Gd-DAD-DiI agent represents the initial goal of this project, and its accomplishment should provide for many useful biological studies involving the development of the central nervous system in vertebrates.

The first test of Gd-DAD-DiI was to investigate whether a developing embryo can function normally once injected with the agent. In an initial trial that is used as a standard

procedure for testing toxicity of imaging agents, a series of chick embryos was injected with 10 ms pulses at 30 psi with a 10 mg/mL solution of Gd-DAD-DiI in DI water in the hindbrain of the neural tube at Hamburger/Hamilton (H/H)[89] Stage 12 and allowed to incubate overnight at 40°C. The following day, all seven embryos had survived and had developed normally to about H/H Stage 17. Six of the seven embryos were fluorescent.

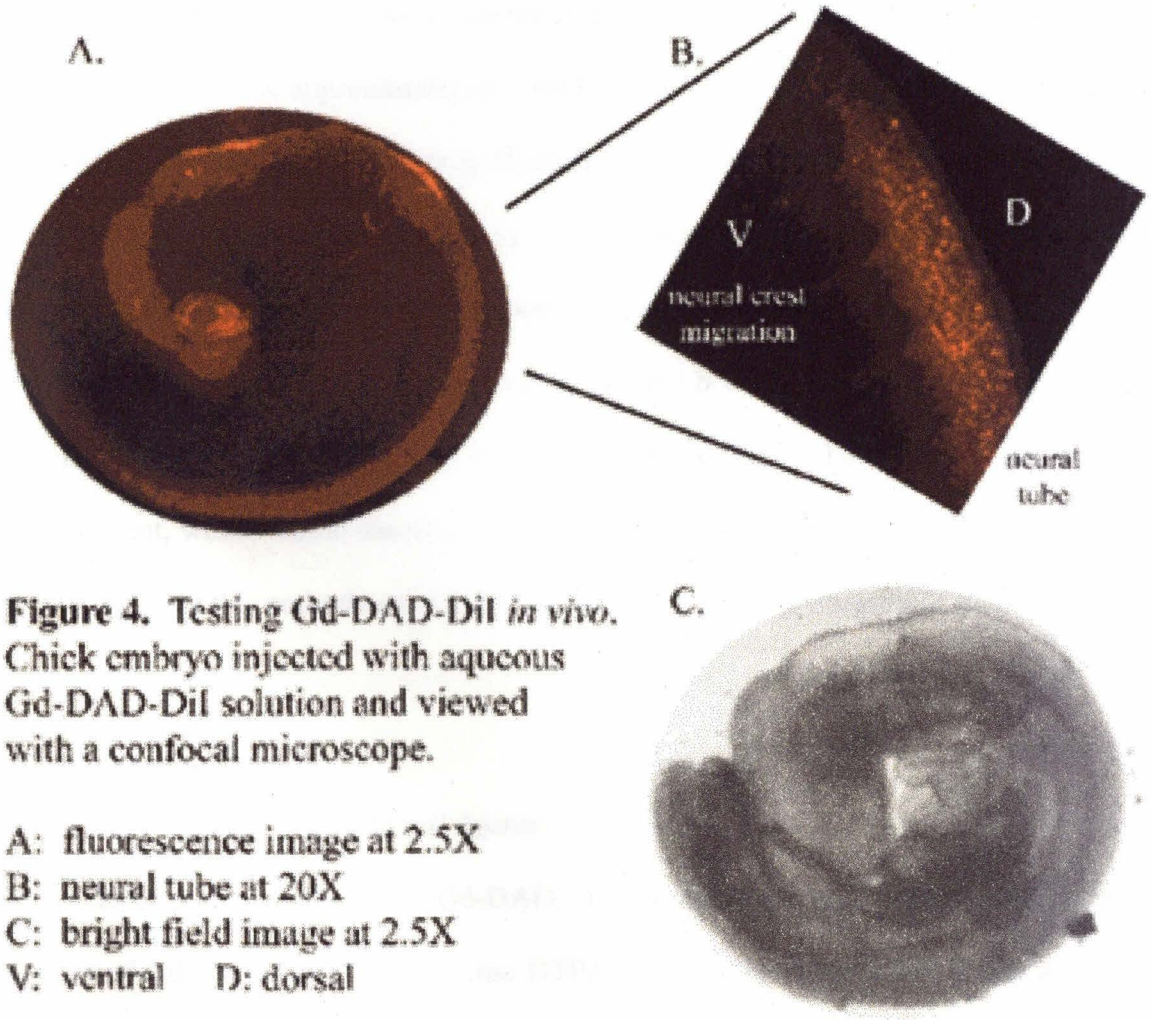

Figure 4. Testing Gd-DAD-DiI *in vivo*. Chick embryo injected with aqueous Gd-DAD-DiI solution and viewed with a confocal microscope.

A: fluorescence image at 2.5X
B: neural tube at 20X
C: bright field image at 2.5X
V: ventral D: dorsal

Figure 4 shows a typical embryo in this study using confocal fluorescence microscopy. The most important observation is that Gd-DAD-DiI is not toxic. This is in

contrast with agents based on the poly-D-lysine scaffold, which exhibited fatal toxicity. Also, Gd-DAD-DiI is readily taken up by cells throughout the neural tube. This can best be seen in Figure 4B, where migration of the neural crest cells can be seen by fluorescence. It is speculated that the agent, due to the impermeability of dextran, is latching onto the outer cell membranes of these cells via alkyl chain infiltration of the DiI.

Measurements of T_1 were carried out with Gd-DAD-DiI, and the relaxivity in water was found to be approximately 6.1 $mM^{-1}s^{-1}$, comparable to that found for the parent Gd-DAD (5.82 $mM^{-1}s^{-1}$). However, preliminary trials to find an MRI signal in the labeled chick embryo after fixation failed in an 11.7 T magnet with a series of different pulse sequences. One explanation for a pronounced T_1 effect in solution but not in the a chick embryo is that, upon fixation, water access is blocked because the agent is tightly adhered to cell membranes. There is also the effect that agent is likely to be diluted during development, which would decrease $1/T_1$ and give a low signal. Future studies will focus on the utility of this and other Gd-DAD based agents for MR imaging in both living and fixed tissue.

3.1.5 Toward Trifunctional Agents

During the synthesis of Gd-DAD, it was observed that even though a large amount of Gd^{3+} was complexed by the DTPA chelates, there were still a few available uncomplexed DTPA units. This was shown as a matter of happenstance by the addition of Eu^{3+} ions to an aqueous solution of Gd-DAD. Since the Eu^{3+} ion does not have a symmetric electronic ground state, it complexes easily at room temperature to DTPA,

whereas Gd^{3+} complexation with $GdCl_3$ takes hours or even several days at 80°C or more. This additional complexation of Eu^{3+} to Gd-DAD was first evidenced by the slow decrease in pH after $EuCl_3$ addition and neutralization, which normally occurs during complexation due to the release of HCl. Purifying the Gd/Eu-DAD species by dialysis and obtaining elemental analysis (C,H,N,Gd,Eu) showed a significant content of Eu in addition to the approximate Gd content already observed for Gd-DAD. Since Eu^{3+} has a longer fluorescence lifetime in aqueous solution than Gd^{3+} (though not as much as most transition metal complexes), Eu^{3+} complexes have found applications in fluorescence microscopy.[90,91] As a result, the new heterobimetallic species Gd/Eu-DAD is already a *bi*functional agent even before attaching an organic fluorophore. This means that a *tri*functional should be accessible through conjugation of a non-imaging agent to the remaining free amine.

With the free amine, a molecule that serves another purpose can be attached. One could conjugate another fluorophore which fluoresces at wavelengths different from Eu-DTPA and obtain a multiwavelength agent that also enhances MRI signals. Or, a completely different function can be served at the free amine. Scheme 12 shows the reaction of the Eu/Gd-DAD species with an amine-reactive form of biotin. Biotin is a stereogenic molecule that selectively binds the polypeptide avidin with a binding affinity stronger than any other naturally occuring noncovalent interaction,[92] making biotin especially useful in molecular targeting applications. Biotin has already been used in studies involving immobilization of polysaccharides.[93] The Eu/Gd-DAD complex was

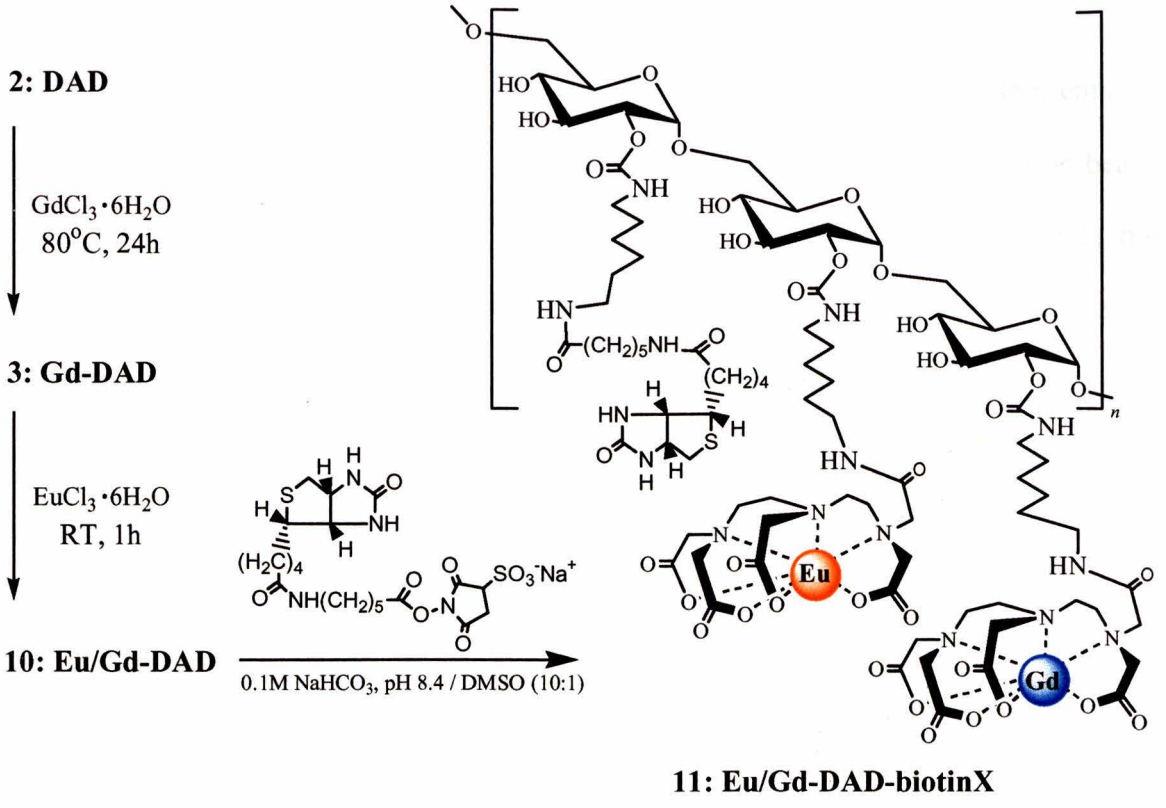

Scheme 12. Heterobimetallation of DAD and subsequent addition of biotin-X to form trifunctional imaging agent.

purified and isolated and characterized based on elemental data. Upon reaction with 6-((biotinoyl)amino)hexanoic acid, sulfosuccinimidyl ester, sodium salt (biotin-X, SSE), the agent was isolated and shown qualitatively to have retained the biotin-X molecule by the HABA-avidin assay.[94-96] In this assay, the chromophoric molecule 2-(4'-hydroxyazobenzene)benzoic acid (HABA), is complexed to the avidin protein, and since biotin has a stronger binding affinity, it displaces the HABA molecule and changes the absorbance in the UV-vis spectrum. However, a small quantity of Eu/Gd-DAD-biotinX was isolated and thus prevented further characterization. Nonetheless, this serves as evidence of a trifuntional agent, and it follows that the Eu/Gd-DAD species would serve as a template for investigating other multifunctional agents.

3.2 MION Particle Conjugates

Multifunctional agents can assume a wide variety of forms. A system entirely distinct from the dextran scaffold is a class of nanometer-scale paramagnetic iron beads called microcrystalline iron oxide nanoparticles (MION particles). As opposed to the Gd^{3+} complexes already described, the MION particles serve as T_2-weighted agents rather than T_1-weighted agents. T_2 agents are relatively unexplored and are not as widely used in clinical applications as T_1-weighted agents. The MION applications will be distinct from the dextran agents since nanometer-sized beads will inherently behave differently in living systems, which may or may not be advantageous. One key advantage of the MION system is that the MRI agent is already in the system, so that only full recovery of the beads during further conjugation is required for 100% yields of the MRI agent. In a *very* preliminary study, a set of carboxy/amino-coated MION particles were conjugated to a fluorophore for fluorescence imaging and concomitantly to biotin for molecular recognition or targeting to the avidin protein. Since the bead supplier recommends always keeping the beads in a minimum 80% aqueous solution, the succinimidyl ester functional group was chosen as the mode of conjugation. The fluorophores tetramethylrhodamine (TR) and Alexa Fluor 568 were chosen for the fluorescence agents. TR is a well characterized and widely used fluorophore, and Alexa Fluor 568 is a member of the new and novel class of two-photon[97] dyes that have recently been reported.[98-100] The MION conjugation with biotin-XX and Alexa Fluor 568 is shown in Scheme 13.

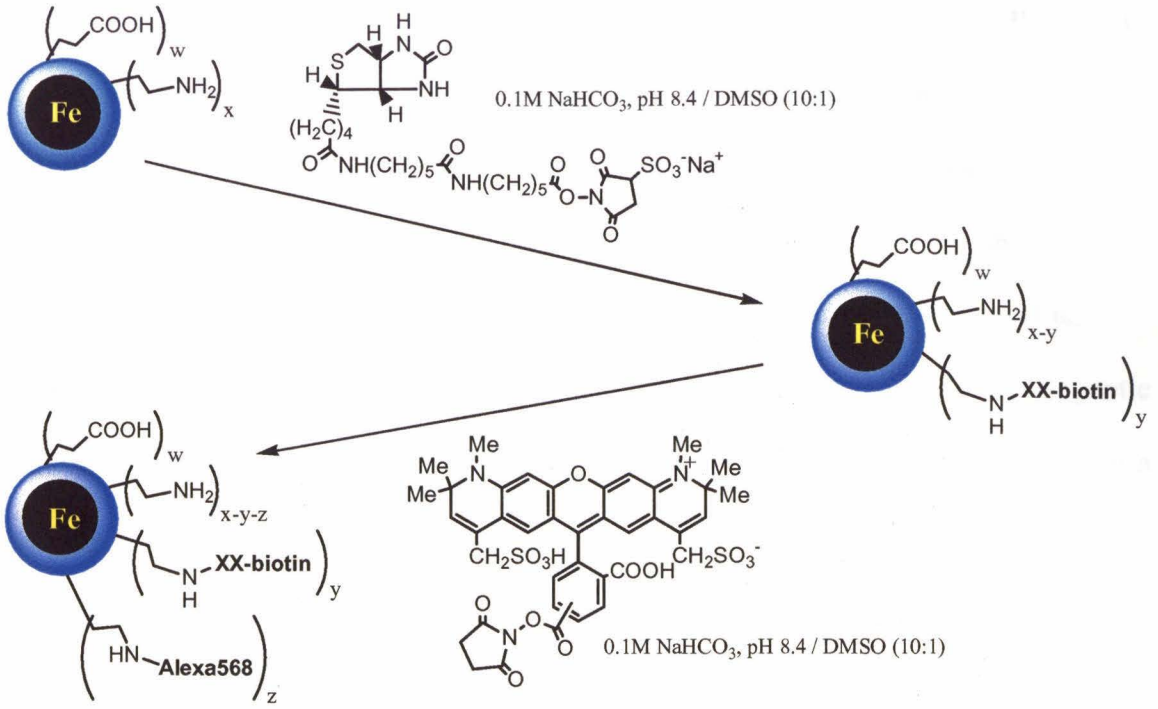

12: [Fe]-biotinXX-AF568

Scheme 13. Conjugation of biotin-XX and Alexa 568 to iron oxide MION particles to make [Fe]-biotinXX-AF568.

An advantage of this dual conjugation is that, after each step, the beads could be purified from the reaction mixture by magnetic filtration (Experimental Section – General Methods) in which the magnetic entities are retained and impurities are washed away. In this study, the final product [Fe]-biotinXX-AF568 was isolated and characterized by HABA-avidin assay for the biotin and by UV-vis and fluorescence spectroscopies for the Alexa Fluor 568. By HABA assay, the biotin molecules were indeed detectable and even quantifiable (in Scheme 13, y = ca. 30,000). The Alexa Fluor 568 was also detectable but very weak in both the UV-vis and fluorescence spectra. Tetramethylrhodamine conjugates also gave positive readings for biotin but weak signals in the UV-vis and fluorescence spectra. It was first speculated that conjugation to relatively macroscopic beads had adversely affected the optical properties of the fluorophore. However, a

secondary hypothesis that the magnetic filtration was somehow not giving full recovery of the iron beads was tested. A series of filtrations was run on the iron beads alone and their T_2 relaxation rates measured in standardized volumes. The filtrations were shown to recover only about one-fifteenth the original iron bead content. The reason the biotin readings were better than the fluorophore was that the MION particles were first isolated from a proprietary buffer with the magnetic filtration system. However, magnetic filtration yielded only one-fifteenth the total particles used. Biotin was then added in a quantity consistent with the original (MION as purchased) quantity of amines present. But since fewer amines than expected were present, biotin was actually added unknowingly in large excess. This reaction presumably labeled nearly all available amines, leaving almost no amines for conjugation to the fluorophore. Future work in this area would first need to address a bead/filtration combination that yields full recovery.

4 Conclusions and Future Directions

Shown in this manuscript is a more detailed approach to synthesizing dextran-based multifunctional conjugates for simultaneous fluorescence and MR imaging. Paying close attention to some of the finer synthetic details of dextran conjugate production has allowed for purer intermediates, higher agent loads, more thorough characterization, and a better idea for what is happening in this complex system than in previous studies.

A series of multifunctional dextran agents has been produced with one type of MR agent (Gd-DTPA) and a range of fluorescent molecules. One future direction for this work would be to vary the MRI agent, perhaps with a T_2-weighted agent or a more rigid system that would exhibit a better tumbling correlation with the macromolecular scaffold

and increase relaxivity. In this latter scenario, the load of MRI agent would not have to be as high, which would ease the constraint of making new multifunctional agents. Another direction would be to explore the targeting capability of the dextran agents. For instance, a molecule such as biotin or one that recognizes certain other protein receptors is tethered to a macromolecular agent with a high payload of MRI agent. With both fluorescence and MRI capabilities on this agent in *large* concentration (multiple units of each imaging moiety), certain *low* concentration proteins or antibodies could be followed both short- and long-term. One similar study would be the attachment of a polypeptide bearing the CAAX (cysteine-aliphatic-aliphatic-variable) sequence, which becomes immobilized in the cytosol by a particular enzyme that recognizes the CAAX sequence. This peptide has been previously conjugated to a dextran Ca^{2+} indicator,[101] and with the knowledge that this conjugate has been immobilized at a known enzyme whose localization has been studied, novel long-term lineage studies could be carried with the added MRI capabilities. This and related experiments open the door to a multitude of variations on the theme of multifunctional agents and what can be learned from them.

5 Experimental Section

General Methods. All aqueous manipulations were carried out in Nanopure water, except for dialysis baths, in which house deionized (DI) water was employed. Dialysis purifications were done using buffer-treated membranes purchased from Spectra/Por; unless indicated otherwise, the molecular weight cut-off (MWCO) was 3500 for each experiment. Amino/carboxy polymer coated ferrofluid was purchased from Immunicon as a colloid of magnetic Fe nanoparticles (110-140nm), conjugated to

roughly 5 x 10^5 amino and carboxy groups per particle and suspended in a proprietary buffer (pH 7.5) containing Bovine Serum Albumin (BSA) and Proclin300. Magnetic filtrations were carried out with μMACS high gradient separation columns and magnetic unit purchased from Miltenyi Biotec. Dextran (MW = 10,500 avg.) and diethylenetriaminepentaacetic (DTPA) dianhydride were purchased from Sigma, and all fluorescent dyes and biotin reagents were bought from Molecular Probes, Inc. All other reagents were widely available from commercial sources and were used without further purification. DMSO was dried and stored over activated 4Å molecular sieves prior to use. Injections into brown chick embryos were performed at Hamburger-Hamilton stage 12 or 13,[89] incubated overnight at 40°C, and viewed by confocal fluorescence microscopy at stage 17 or 18.

Instrumentation. ^1H, ^{13}C, and ^{31}P NMR spectra were obtained on a Varian Mercury spectrometer at 300, 75.5, and 123 MHz, respectively. Elemental analyses were carried out at Desert Analytics Laboratory in Tuscon, Arizona. Mass spectrometry was performed by electrospray (ESI) ionization, quadrupole mass spectrometry in the PPMAL – Protein/Peptide MicroAnalytical Laboratory, Beckman Institute, California Institute of Technology. FTIR samples were analyzed as nujol mulls on a Perkin Elmer 1600 series FTIR spectrophotometer. Thin-layer chromatography was performed on aluminum-backed 0.2mm-thick silica gel 60 F_{254} (Merck) and was analyzed with a 254nm- and 365nm lamp. UV-vis spectra were obtained with a Hewlett-Packard diode array spectrophotometer with cell temperature maintained at 22.0°C. Fluorescence spectra were recorded on a Hitachi F-4500 fluorescence spectrophotometer. Conductivity measurements were carried out with a Bio-Rad conductivity monitor

referenced to house deionized water. Longitudinal water proton relaxation rates (T_1) were measured at 60 MHz by using a Bruker mq60 NMR Analyzer (Bruker Canada, Milton, Ont. Canada) operating at 1.5 T, by means of the standard inversion-recovery technique (10 data points, 8 scans each). A typical 90°-pulse length was 6.16μs, and the reproducibility of the T_1 data was ±0.3%. The temperature was maintained by the instrument at 40°C, and all samples were prepared in buffer containing 10mM 3-[N-morpholino]propanesulfonic acid (MOPS) and 100mM NaCl at pH 7.4. Confocal fluorescence microscopy was carried out on a Zeiss 410 confocal microscope (Serial No. 840091).

DexAm (1). Dextran (2.30 g, 14.2 mmol based on Glu monomers) was weighed into a 3-neck, 2L round-bottom flask with stirrer. 800 mL of water was added, and the mixture was stirred for 15 minutes. The solution pH was adjusted to 10.7 with dropwise addition of NaOH (0.15 N). BrCN (1.05 g, 9.91 mmol, 0.7 equiv. based on Glu monomers) was added by rinsing with water through a pressure-equilized addition funnel at about one drop per second. After addition, thepH was maintained between 10.4 and 10.7 by addition of 0.15N NaOH. After 4 hours from the start of BrCN addition, the pH was adjusted to 7.8 with HCl (0.10 N), and 1,6-diaminohexane (2.47 g, 21.3 mmol) was added at once as a solid. The solution was allowed to stir further for two hours. The solution was concentrated from about 1300 mL to 100 mL by rotary evaporation and purified through dialysis. The aqueous supernatant bath was monitored by UV-vis spectroscopy, and about 6 bath changes (every 12 hours) with DI water were sufficient. DexAm solution was collected in 250mL one-neck round bottom flask and concentrated

to 50 mL by rotary evaporation and lyophilized, giving DexAm as a fluffy, white powder. Yield: 2.14 g. DexAm: C, 41.88%; H, 6.46%; N, 2.68%. ^{1}H NMR (D_2O): δ = 1.20 (br), 1.41 (br), 2.65 (br), 3.3 - 3.8 (m), 4.83 (d); ^{13}C NMR (D_2O): δ = 25.7 (br), 28.2 (br), 39.8 (br), 60.6 (br), 65.6 (s), 69.6 (s), 70.3 (s), 71.5 (s), 73.5 (s), 97.8 (s); IR (nujol mull): ν(carbamate) = 1713 (C=O), 1230 (C-N) cm^{-1}.

DexAmDTPA (DAD) (2). DexAm (830 mg) was weighed into a 3-neck, 1L round-bottom flask with stirrer. The flask was stoppered, evacuated and purged with Ar twice, and 210mL dry DMSO was added. A suspension formed, and most or all of the DexAm went into solution after 30 minutes. DTPA dianhydride (5.0g, 14.0mmol) in 100mL dry DMSO was added via addition funnel over 10 minutes. The resulting yellow solution was allowed to stir for 12 hours. 50mL water was added, and the solution was allowed to stir 30 minutes. The solution was filtered through a course glass-sintered frit and loaded into dialysis bags large enough to hold 3 times the volume (influx of supernatant water). Aqueous supernatant bath was changed every 12 hours with DI water and was monitored by scent, pH, and finally UV-vis spectroscopy until pH steadied and UV-vis signal vanished (about 7 bath changes). The solution was collected in a 2L flask and concentrated to about 50mL by rotary evaporation and lyophilized, giving DexAmDTPA as an off-white powder. Yield: 862mg. DexAmDTPA: C, 36.4%; H, 5.38%; N, 8.08%.

GdDexAmDTPA (Gd-DAD) (3). DexAmDTPA (850mg) was weighed into a one-neck 250mL round-bottom flask with stirrer. 150mL water was added, and the

solution was allowed to stir 15 minutes. A 20mL aqueous solution of $GdCl_3 \cdot 6H_2O$ (2.20g, 5.92mmol) was added all at once. The pH was adjusted to 6.0 with 0.15N NaOH, bringing the total volume to 200mL, and the flask was fitted with a reflux condenser and heated to 80°C for 24 hours under Ar. The solution was allowed to cool and was purified by dialysis. The supernatant bath was monitored by a combination of UV-vis spectroscopy, conductivity, and T_1 until no Gd^{3+} was detected (about 5 bath changes). The retained solution was collected and concentrated to about 30mL by rotary evaporation and lyophilized, giving GdDexAmDTPA as a fluffy, white powder. Yield: 871mg. Gd-DAD: C, 37.5%; H, 5.68%; N, 2.86%; Gd, 6.86%. Relaxivity: 2539.8 $(g/mL)^{-1}s^{-1}$ (based on mass of sample) = 5.82 $mM^{-1}s^{-1}$ (based on molarity of Gd content, as computed from elemental data).

GRID (4). Gd-DAD (216mg) was weighed into a 2-neck 100mL round-bottom flask with stirrer. The sealed flask was evacuated and purged with Ar twice. 10mL dry DMSO was added, and the suspension was allowed to stir for 10 minutes. Dry pyridine (58μL) and dibutyltin dilaurate (35μL) were added via pipet against a backflow of Ar, and the suspension was heated. The suspension dissolved completely at about 70°C, yielding a yellowish solution. Tetramethylrhodamine-5(and-6)-isothiocyanate (5(6)-TRITC) (30mg, 0.067mmol) in 30mL dry DMSO was added dropwise through an addition funnel. The deep-red solution was heated further to 80°C and allowed to stir for 15 hours in the absence of light. The solution was allowed to cool and was loaded into dialysis bags large enough to hold 3 times the volume (influx of supernatant water). While constantly protected from light, the supernatant bath was changed frequently with

DI water and was monitored by observation of color (pink) and finally by UV-vis spectroscopy. The retained solution was collected and filtered through a medium glass-sintered frit. The filtrate was concentrated to 15mL by rotary evaporation and lyophilized to give a red powder. Yield: 240mg. GRID: C, 41.87%; H, 6.35%; N, 2.77%; Gd, 5.20%; S, 1.25%.

Gd-DAD-Fl (5), Gd-DAD-Py (6). Analogous procedures to making GRID were employed with the isothiocyanate derivatives fluorescein-6-isothiocyanate (6-FITC) and 1-pyreneisothiocyanate (1-PyITC), respectively.

Gd-DAD-OG488 (8). Gd-DAD (40mg) was stirred in 4.0mL 0.1M $NaHCO_3$ at pH 8.4 for 15 minutes in a 20mL scintillation vial. A solution of Oregon Green™ 488-6-carboxylic acid, succinimidyl ester (6-OG488SE) (5mg, 9.8μmol) in dry DMSO (0.5mL) was added dropwise. The orange solution was stirred at RT for 1 hour and subsequently purified by dialysis. The dialysis bath was monitored by UV-vis spectroscopy and required about 8 changes with DI water over three days. The solution was then filtered through a fine glass-sintered frit and lyophilized to give an orange powder. Yield: 37mg.

Gd-DAD-AF568 (7). Analogous procedure to making Gd-DAD-OG488 was employed with Alexa Fluor 568 carboxylic acid, succinimidyl ester (AF568SE) (0.32mg, 0.81μmol) and Gd-DAD (30mg). Yield: 20.6 mg.

Gd-DAD-DiI (9). Gd-DAD (30mg) and K_2CO_3 (0.7mg, 2 equiv. based on dye) were weighed into a one-neck 20mL round-bottom flask with stirrer. 5-[(4-chloromethyl-benzoylamino)-methyl]-DiI (CM-DiI) (5mg, 0.0048mmol) was added as a dry DMSO solution (2mL). The flask was evacuated and purged with Ar twice and then heated to 80°C in the absence of light. The reaction was monitored by TLC with KNO_3(sat.)/H_2O/CH_3CN (1:6:93) as the mobile phase until the disappearance of the CM-DiI spot ($R_f = 0.42$). After 22 hours, only the dextran conjugate spot ($R_f = 0$) and several decomposition spots remained. The solution was cooled and loaded into dialysis. With constant protection from light, the supernatant bath was changed frequently with DI water and was monitored by UV-vis spectroscopy (about 5 bath changes). The retained solution was collected and filtered through a fine porosity glass-sintered frit. The filtrate was concentrated to 5mL by rotary evaporation and lyophilized to give a pink-purple powder. Yield: 23mg.

Gd/Eu-DAD (10). DexAmDTPA (300mg) was weighed into a one-neck 250mL round-bottom flask with stirrer. 50mL water was added, and the solution was allowed to stir 15 minutes. A 10mL aqueous solution of $GdCl_3 \cdot 6H_2O$ (103mg, 0.276mmol, a *sub*cess based on DTPA units calculated from elemental data on DexAmDTPA) was added all at once. The pH was adjusted to 6.0 with 0.15N NaOH, and the flask was fitted with a reflux condenser and heated to 80°C for 15 hours under Ar. The solution was allowed to cool to 40°C, and $EuCl_3 \cdot 6H2O$ (109mg, 0.299mmol, an excess of the remaining DTPA ligands) in 10mL H_2O was added. The pH was adjusted to 6.0, and the solution was allowed to stir and cool to RT for one hour. The product was purified by

dialysis and the supernatant bath was monitored by conductivity until no ions were detected (about 5 bath changes). The retained solution was collected and pumped to dryness by rotary evaporation, giving Gd/Eu-DAD as shiny yellow flakes. Yield: 190mg. Gd/Eu-DAD: C, 29.5%; H, 4.47%; N, 6.09%; Gd, 8.51%; Eu, 7.81%.

Gd/Eu-DAD-biotinX (11). Eu/Gd-DAD (91mg) was stirred in 8.0mL 0.1M $NaHCO_3$ at pH 8.4 for 15 minutes in a 20mL scintillation vial. A dry DMSO solution (1.0mL) of 6-((biotinoyl)amino)hexanoic acid, sulfosuccinimidyl ester, sodium salt (biotin-X, SSE) (10.0mg, 17.9μmol) was added dropwise, and the resulting light yellow solution was stirred 1 hour and then purified by dialysis. The supernatant bath was monitored by UV-vis spectroscopy until no biotin-X was detectable (7 changes over 4 days). The dialyzed solution was collected, filtered, and dried by rotary evaporation to give an off-white powder. Yield: 12 mg.

[Fe]-biotinXX-AF568 (12). Amino/carboxy polymer coated ferrofluid (0.750mL, 1.2×10^{-7} mol $-NH_2$) was separated from the proprietary buffer by magnetic filtration and taken into a 10mL round-bottom flask *without stirrer* with 1.50mL 0.1M $NaHCO_3$ buffer at pH 8.4. The flask was loaded onto a Mini Vortexer (VWR Scientific Products) set at continuous gentle vibration. 6-((6-((biotinoyl)amino)hexanoyl)amino)hexanoic acid, sulfosuccinimidyl ester, sodium salt (biotin-XX, SSE) (0.0017mg, 2.5×10^{-9} mol) was added as a dry DMSO solution (0.150mL), and the colloid was stirred by vortex for one hour. The biotinylated particles were purified by magnetic filtration and taken into the same flask with 1.50mL fresh bicarbonate buffer. With gentle vibration, Alexa Fluor

568, carboxylic acid, succinimidyl ester (0.32mg, 0.81μmol) was added as a dry DMSO solution (0.100mL), and the colloid was stirred by vortex for one hour. The doubly labeled particles were purified by magnet filtration and taken into the original proprietary buffer (0.750mL) and 0.750 of additional bicarbonate buffer.

6 References

1. Kalyani AJ, Rao MS: **Cell lineage in the developing neural tube.** *Biochem. Cell Biol.* 1998, **76**:1051-1068.
2. Clarke JDW, Tickle C: **Fate maps old and new.** *Nat. Cell Biol.* 1999, **1**:E103-E109.
3. Sieber-Blum M: **Factors controlling lineage specification in the neural crest.** *Int. Rev. Cytol.* 2000, **197**:1-33.
4. Sulston JE, Horvitz HR: **Post-embryonic cell lineages of the nematode, *Caenorhabditis elegans*.** *Dev. Biol.* 1977, **56**:110-156.
5. Kimble J, Hirsh D: **The postembryonic cell lineages of the hermaphrodite and male gonads in *Caenorhabditis elegans*.** *Dev. Biol.* 1979, **70**:396-417.
6. Sulston JE, Schierenberg E, White JG, Thomson JN: **The embryonic cell lineage of the nematode *Caenorhabditis elegans*.** *Dev. Biol.* 1983, **100**:64-119.
7. Greenwald IS, Sternberg PW, Horvitz HR: **The *lin*-12 locus specifies cell fates in *Caenorhabditis elegans*.** *Cell* 1983, **34**:435-444.
8. Hedgecock EM: **Cell lineage mutants in the nematode *Caenorhabditis elegans*.** *Trends Neurosci.* 1985, **8**:288-293.
9. Jacobs RE, Fraser SE: **Magnetic resonance microscopy of embryonic cell lineages and movements.** *Science* 1994, **263**:681-684.
10. Inoué S: **Foundations of Confocal Scanned Imaging in Light Microscopy.** In *Handbook of Biological Confocal Microscopy*, edn 2. Edited by Pawley JB: Plenum Press; 1995:1-17.
11. Moats RA, Fraser SE, Meade TJ: **A "smart" magnetic resonance imaging agent that reports on specific enzymic activity.** *Angew. Chem., Int. Ed. Engl.* 1997, **36**:726-728.
12. Maus M, Rurack K: **Monitoring pH and solvent proticity with donor-acceptor-substituted biphenyls: a new approach towards highly sensitive and powerful fluorescent probes by tuning the molecular structure.** *New J. Chem.* 2000, **24**:677-686.
13. Rurack K, Kollmannsberger M, Daub J: **Molecular switching in the near infrared (NIR) with a functionalized boron-dipyrromethene dye.** *Angew. Chem., Int. Ed.* 2001, **40**:385-387.
14. Louie AY, Meade TJ: **Recent advances in MRI: novel contrast agents shed light on *in vivo* biochemistry.** *New Technol. Life Sci.: Trends Guide* 2000:7-11.
15. Kohen E, Thorell B, Hirschberg JG, Wouters AW, Kohen C, Bartick P, Salmon JM, Viallet P, Schachtschabel DO, Rabinovitch A, et al.: **Microspectrofluorometric procedures and their applications in biological systems.** In *Modern Fluorescence Spectroscopy.* Edited by Wehry EL: Plenum; 1981:295-346. vol 3.]
16. Taylor DL, Salmon ED: **Basic Fluorescence Microscopy.** In *Methods in Cell Biology.* Edited by Taylor DL: Academic Press, Inc.; 1989:207-237. vol 29.]
17. Farinas J, Verkman AS: **Receptor-mediated targeting of fluorescent probes in living cells.** *J. Biol. Chem.* 1999, **274**:7603-7606.
18. Tsien RY: **Fluorescent and photochemical probes of dynamic biochemical signals inside living cells.** *ACS Symp. Ser.* 1993, **538**:130-146.
19. Pawley JB: **Fundamental Limits in Confocal Microscopy.** In *Handbook of Biological Confocal Microscopy*, edn 2. Edited by Pawley JB: Plenum Press; 1995:19-37.

20. Gustafsson MGL: **Extended resolution fluorescence microscopy**. *Curr. Opin. Struct. Biol.* 1999, **9**:627-634.
21. Gustafsson MGL: **Surpassing the lateral resolution limit by a factor of two using structured illumination microscopy**. *J. Microsc. (Oxford)* 2000, **198**:82-87.
22. Jacobs RE, Ahrens ET, Meade TJ, Fraser SE: **Looking deeper into vertebrate development**. *TIBC* 1999, **9**:73-76.
23. Tweedle MF, Kumar K: **Magnetic resonance imaging (MRI) contrast agents**. *Top. Biol. Inorg. Chem.* 1999, **2**:1-43.
24. Mody TD, Sessler JL: **Chapter 7: Porphyrin- and Expanded Porphyrin-based Diagnostic and Therapeutic Agents**. In *Supromolecular Technology*. Edited by Reinhoudt DN: John Wiley & Sons Ltd.; 1999.
25. Caravan P, Ellison JJ, McMurry TJ, Lauffer RB: **Gadolinium(III) chelates as MRI contrast agents: Structure, dynamics, and applications**. *Chem. Rev.* 1999, **99**:2293-2352.
26. Aime S, Botta M, Fasano M, Terreno E, Kinchesh P, Calabi L, Paleari L: **A new ytterbium chelate as contrast agent in chemical shift imaging and temperature sensitive probe for MR spectroscopy**. *Magn. Reson. Med.* 1996, **35**:648-651.
27. Auteri FP, Chato JC, Kuriashkin I, Eum JSM, Clarkson RB: **Highly sensitive temperature indicating MRI contrast agents using stable paramagnetic nitroxide molecules**. *BED (Am. Soc. Mech. Eng.)* 1995, **29**:377-378.
28. Rohovec J, Lukes I, Hermann P: **Lanthanide complexes of a cyclen derivative with phenylphosphinic pendant arms for possible 1H and 31P MRI temperature sensitive probes**. *New J. Chem.* 1999, **23**:1129-1132.
29. Hall J, Haner R, Aime S, Botta M, Faulkner S, Parker D, de Sousa AS: **Relaxometric and luminescence behavior of triaquahexaazamacrocyclic complexes, the gadolinium complex displaying a high relaxivity with a pronounced pH dependence**. *New J. Chem.* 1998, **22**:627-631.
30. Mikawa M, Miwa N, Brautigam M, Akaike T, Maruyama A: **A pH-sensitive contrast agent for functional magnetic resonance imaging (MRI)**. *Chem. Lett.* 1998:693-694.
31. Aime S, Crich SG, Botta M, Giovenzana G, Palmisano G, Sisti M: **A macromolecular Gd(III) complex as pH-responsive relaxometric probe for MRI applications**. *Chem. Commun. (Cambridge)* 1999:1577-1578.
32. Zhang S, Wu K, Sherry AD: **A novel pH-sensitive MRI contrast agent**. *Angew. Chem., Int. Ed.* 1999, **38**:3192-3194.
33. Mikawa M, Miwa N, Brautigam M, Akaike T, Maruyama A: **Gd3+-loaded polyion complex for pH depiction with magnetic resonance imaging**. *J. Biomed. Mater. Res.* 2000, **49**:390-395.
34. Hovland R, Glogard C, Aasen AJ, Klaveness J: **Gadolinium DO3A derivatives mimicking phospholipids; preparation and in vitro evaluation as pH responsive MRI contrast agents**. *J. Chem. Soc., Perkin Trans. 2* 2001:929-933.
35. Lowe MP, Parker D: **Controllable pH modulation of lanthanide luminescence by intramolecular switching of the hydration state**. *Chem. Commun. (Cambridge)* 2000:707-708.
36. Li W-h, Fraser SE, Meade TJ: **A Calcium-Sensitive Magnetic Resonance Imaging Contrast Agent**. *J. Am. Chem. Soc.* 1999, **121**:1413-1414.
37. Louie AY, Huber MM, Ahrens ET, Rothbacher U, Moats R, Jacobs RE, Fraser SE, Meade TJ: ***In vivo* visualization of gene expression using magnetic resonance imaging**. *Nat. Biotechnol.* 2000, **18**:321-325.
38. Lemieux GA, Yarema KJ, Jacobs CL, Bertozzi CR: **Exploiting differences in sialoside expression for selective targeting of MRI contrast reagents**. *J. Am. Chem. Soc.* 1999, **121**:4278-4279.
39. Bhorade R, Weissleder R, Nakakoshi T, Moore A, Tung C-H: **Macrocyclic Chelators with Paramagnetic Cations Are Internalized into Mammalian Cells via a HIV-Tat Derived Membrane Translocation Peptide**. *Bioconjugate Chem.* 2000, **11**:301-305.
40. Kuhn W: **NMR microscopy - fundamentals, limits, and possible applications**. *Angew. Chem., Int. Ed.* 1990, **29**:1-19.
41. Schneider G, Seidel R, Uder M, Wagner D, Weinmann H-J, Kramann B: **In vivo microscopic evaluation of the microvascular behavior of FITC-labeled macromolecular MR contrast agents in the hamster skinfold chamber**. *Invest. Radiol.* 2000, **35**:564-570.

42. Hüber MM, Staubli AB, Kustedjo K, Gray MHB, Shih J, Fraser SE, Jacobs RE, Meade TJ: **Fluorescently Detectable Magnetic Resonance Imaging Agents**. *Bioconjugate Chem.* 1998, **9**:242-249.
43. Mann JS, Huang JC, Keana JFW: **Molecular amplifiers: synthesis and functionalization of a poly(aminopropyl)dextran bearing a uniquely reactive terminus for univalent attachment to biomolecules**. *Bioconjugate Chem.* 1992, **3**:154-159.
44. Keana JFW, Mann JS: **Chelating ligands functionalized for facile attachment to biomolecules. A convenient route to 4-isothiocyanatobenzyl derivatives of diethylenetriaminepentaacetic acid and ethylenediaminetetraacetic acid**. *J. Org. Chem.* 1990, **55**:2868-2871.
45. Brechbiel MW, Gansow OA: **Backbone-substituted DTPA ligands for yttrium-90 radioimmunotherapy**. *Bioconjugate Chem.* 1991, **2**:187-194.
46. Brandt KD, Johnson DK: **Structure-function relationships in indium-111 radioimmunoconjugates**. *Bioconjugate Chem.* 1992, **3**:118-125.
47. Hashifuchi Y, Iwai K, Seri S, Kondo S, Azuma M: **Preparation of bifunctional ligands for metals as imaging agent for diagnosis**. US Patent 1993, 535668.
48. Cheng RC-L: **Process for preparing macrocyclic chelating agents and formation of chelates and conjugates thereof**. US Patent 1996, 9607435.
49. Li M, Selvin PR: **Amine-Reactive Forms of a Luminescent Diethylenetriaminepentaacetic Acid Chelate of Terbium and Europium: Attachment to DNA and Energy Transfer Measurements**. *Bioconjugate Chem.* 1997, **8**:127-132.
50. Takenouchi K, Tabe M, Watanabe K, Hazato A, Kato Y, Shionoya M, Koike T, Kimura E: **Novel pendant-type macrocyclic bifunctional chelating agents: (carboxymethyl)amino derivatives of 2-(4-nitrobenzyl)-1,4,7,10-tetraazacyclododecane-N,N',N'',N'''-tetraacetic acid and their complex formation with yttrium(III)**. *J. Org. Chem.* 1993, **58**:6895-6899.
51. Takenouchi K, Watanabe K, Kato Y, Koike T, Kimura E: **Novel bifunctional macrocyclic chelating agents appended with a pendant-type carboxymethylamino ligand and nitrobenzyl group and stability of the 88YIII complexes**. *J. Org. Chem.* 1993, **58**:1955-1958.
52. Meade TJ, Fraser SE, Jacobs RE: **Bifunctional detection agents having a polymer covalently linked to an MRI agent and an optical dye**. US Patent 1999, 5900228.
53. Wiener EC, Brechbiel MW, Brothers H, Magin RL, Gansow OA, Tomalia DA, Lauterbur PC: **Dendrimer-based metal chelates: a new class of magnetic resonance imaging contrast agents**. *Magn. Reson. Med.* 1994, **31**:1-8.
54. Wiener EC, Brechbiel MW, Gansow OA, Foley G, Lauterbur PC: **Dendrimer-based contrast agents for diagnostic imaging**. *Polym. Mater. Sci. Eng.* 1997, **77**:193-194.
55. Duarte MG, Gil MH, Peters JA, Colet JM, Vander Elst L, Muller RN, Geraldes CFGC: **Synthesis, Characterization, and Relaxivity of Two Linear Gd(DTPA)-Polymer Conjugates**. *Bioconjugate Chem.* 2001, **12**:170-177.
56. Fukui K, Moriyama T, Miyake Y, Mizutani K, Tanaka O: **Purification and properties of glucosyltransferase responsible for water-insoluble glucan synthesis from Streptococcus mutans**. *Infect. Immun.* 1982, **37**:1-9.
57. Zhao Q, Gottschalk I, Carlsson J, Arvidsson L-E, Oscarsson S, Medin A, Ersson B, Janson J-C: **Preparation and Purification of an End to End Coupled mEGF-Dextran Conjugate**. *Bioconjugate Chem.* 1997, **8**:927-934.
58. Vandoorne F, Bruneel D, Vercauteren R, Schacht E: **New approach to dextran derivatives containing primary amino functions**. *Makromol. Chem.* 1991, **192**:673-677.
59. Ramirez JC, Sanchez-Chaves M, Arranz F: **Dextran functionalized by cyclic carbonate groups as supports of bioactive compounds**. *Angew. Makromol. Chem.* 1993, **206**:77-85.
60. Ramirez JC, Sanchez-Chaves M, Arranz F: **Dextran functionalized by 4-nitrophenyl carbonate groups. Aminolysis reactions**. *Angew. Makromol. Chem.* 1995, **225**:123-130.
61. Shafer DE, Toll B, Schuman RF, Nelson BL, Mond JJ, Lees A: **Activation of soluble polysaccharides with 1-cyano-4-dimethylaminopyridinium tetrafluoroborate (CDAP) for use in protein-polysaccharide conjugate vaccines and immunological reagents. II. Selective crosslinking of proteins to CDAP-activated polysaccharides**. *Vaccine* 2000, **18**:1273-1281.
62. Wongkhalaung C, Kashiwagi Y, Magae Y, Ohta T, Sasaki T: **Cellulase immobilized on a soluble polymer**. *Appl. Microbiol. Biotechnol.* 1985, **21**:37-41.

63. Abdel-Naby MA: **Catalytic properties of stabilized cellobiase by covalent coupling to soluble polysaccharide.** *Afr. J. Mycol. Biotechnol.* 1998, **6**:65-74.
64. Abdel-Naby MA: **Stabilization of cellobiase by covalent coupling to soluble polysaccharide.** *Microbiol. Res.* 1999, **154**:213-218.
65. Veysi Baki A, Vaughan K: **Functional-group modifications of dextran for linkage to a diazonium group. A potential vehicle for tumor targeting of antineoplastic triazenes.** *Carbohydr. Res.* 1982, **105**:57-68.
66. Takakura Y, Kaneko Y, Fujita T, Hashida M, Maeda H, Sezaki H: **Control of pharmaceutical properties of soybean trypsin inhibitor by conjugation with dextran I: synthesis and characterization.** *J. Pharm. Sci.* 1989, **78**:117-121.
67. Molteni L, Scrollini F: **Method of prolonging the activity of drugs by formation of macromolecular compounds.** *Eur. J. Med. Chem. - Chim. Ther.* 1974, **9**:618-620.
68. Molteni L, Antonini E, Trebbi A: **Amino group-containing pharmaceuticals of prolonged action.** US Patent 1974, 2413512.
69. Kim DS, Jung YJ, Kim YM: **Synthesis and properties of dextran-linked ampicillin.** *Drug Dev. Ind. Pharm.* 2001, **27**:97-101.
70. Liberda J, Ticha M, Jonakova V: **Preparation of fluorescein-labeled and biotinylated derivatives of polysaccharides for lectin-saccharide binding studies.** *Biotechnol. Tech.* 1997, **11**:265-267.
71. Bligh SWA, Harding CT, Sadler PJ, Bulman RA, Bydder GM, Pennock JM, Kelly JD, Latham IA, Marriott JA: **Use of paramagnetic chelated metal derivatives of polysaccharides and spin-labeled polysaccharides as contrast agents in magnetic resonance imaging.** *Magn. Reson. Med.* 1991, **17**:516-532.
72. Castell JV, Cervera M, Marco R: **A convenient micromethod for the assay of primary amines and proteins with fluorescamine. A reexamination of the conditions of reaction.** *Anal. Biochem.* 1979, **99**:379-391.
73. Imai K, Watanabe Y, Toyooka T: **Fluorometric assay of amino acids and amines by use of 7-fluoro-4-nitrobenzo-2-oxa-1,3-diazole (NBD-F) in high-performance liquid chromatography.** *Chromatographia* 1982, **16**:214-215.
74. Lin J-K, Lai C-C: **High performance liquid chromatographic determination of naturally occurring primary and secondary amines with dabsyl chloride.** *Anal. Chem.* 1980, **52**:630-635.
75. Ho C-H, Hlady V, Hu C-Z, Dolence EK: **Fluorescence assay for primary amines on modified polymer surfaces using TIRF spectroscopy.** *Polym. Prepr. (Am. Chem. Soc., Div. Polym. Chem.)* 1995, **36**:127-128.
76. Moore S: **Amino acid analysis: aqueous dimethyl sulfoxide as solvent for the ninhydrin reaction.** *J. Biol. Chem.* 1968, **243**:6281-6283.
77. D'Aniello A, D'Onofrio G, Pischetola M, Strazzullo L: **Effect of various substances on the colorimetric amino acid-ninhydrin reaction.** *Anal. Biochem.* 1985, **144**:610-611.
78. Sheng S, Kraft JJ, Schuster SM: **A specific quantitative colorimetric assay for L-asparagine.** *Anal. Biochem.* 1993, **211**:242-249.
79. Weigele M, DeBernardo SL, Tengi JP, Leimgruber W: **Novel reagent for the fluorometric assay of primary amines.** *J. Amer. Chem. Soc.* 1972, **94**:5927-5928.
80. Udenfriend S, Stein S, Boehlen P, Dairman W, Leimgruber W, Weigele M: **Fluorescamine. Reagent for assay of amino acids, peptides, proteins, and primary amines in the picomole range.** *Science* 1972, **178**:871-872.
81. Pretsch E, Simon W, Seibl J, Clerc T: *Tables of Spectral Data for Structure Determination of Organic Compounds* edn 2. Edited by West T. Berlin: Springer-Verlag; 1989.
82. Gouin S, Winnik FM: **Quantitative assays of the amount of diethylenetriaminepentaacetic acid conjugated to water-soluble polymers using isothermal titration calorimetry and colorimetry.** *Bioconjugate Chem.* 2001, **12**:372-377.
83. Aime S, Botta M, Panero M, Grandi M, Uggeri F: **Inclusion complexes between .beta.-cyclodextrin and .beta.-benzyloxy-.alpha.-propionic derivatives of paramagnetic DOTA- and DTPA-gadolinium(III) complexes.** *Magn. Reson. Chem.* 1991, **29**:923-927.
84. Shukla RB, Kumar K, Weber R, Zhang X, Tweedle MF: **Alteration of electronic relaxation in MR contrast agents through de-novo ligand design.** *Acta Radiologica* 1997, **38**:121-123.
85. Bloembergen N: **Proton relaxation times in paramagnetic solutions.** *J. Chem. Phys.* 1957, **27**:572-573.

86. Haugland RP: *Handbook of Fluorescent Probes and Research Chemicals* edn Sixth. Edited by Spence MTZ. Eugene, OR: Molecular Probes, Inc.; 1996.
87. Leung W-Y, Haugland RP, Mao F: **Lipophilic cyanine dyes with enhanced solubility in aqueous media, and their use in staining biological membranes**. US Patent 1999, 6004536.
88. Aime S, Gianolio E, Terreno E, Giovenzana GB, Pagliarin R, Sisti M, Palmisano G, Botta M, Lowe MP, Parker D: **Ternary Gd(III)L-HSA adducts: evidence for the replacement of inner-sphere water molecules by coordinating groups of the protein. Implications for the design of contrast agents for MRI**. *JBIC, J. Biol. Inorg. Chem.* 2000, **5**:488-497.
89. Hamburger V, Hamilton HL: **A series of normal stages in the development of the chick embryo**. *J. Morphol.* 1951, **88**:49-92.
90. Horrocks WD, Jr., Sudnick DR: **Lanthanide ion probes of structure in biology. Laser-induced luminescence decay constants provide a direct measure of the number of metal-coordinated water molecules**. *J. Am. Chem. Soc.* 1979, **101**:334-340.
91. Horrocks WD, Jr., Sudnick DR: **Lanthanide ion luminescence probes of the structure of biological macromolecules**. *Acc. Chem. Res.* 1981, **14**:384-392.
92. Savage MD: **An introduction to avidin-biotin technology and options for biotinylation**. *BioMethods (Basel)* 1996, **7**:1-29.
93. Priem B, Chambat G, Ruel K, Joseleau J-P: **Use of the avidin-biotin complex for specific immobilization of xyloglucan polysaccharides**. *J. Carbohydr. Chem.* 1997, **16**:625-633.
94. Green NM: **A spectrophotometric assay for avidin and biotin based on binding of dyes by avidin**. *Biochem. J.* 1965, **94**:23c-24c.
95. Green NM: **Spectrophotometric Determination of Avidin and Biotin**. *Methods Enzymol.* 1970, **18**:418-424.
96. Livnah O, Bayer EA, Wilchek M, Sussman JL: **The structure of the complex between avidin and the dye, 2-(4'- hydroxyazobenzene) benzoic acid (HABA)**. *FEBS Lett.* 1993, **328**:165-168.
97. So PTC, Dong CY, Masters BR, Berland KM: **Two-photon excitation fluorescence microscopy**. *Annu. Rev. Biomed. Eng.* 2000, **2**:399-429.
98. Panchuk-Voloshina N, Haugland RP, Bishop-Stewart J, Bhalgat MK, Millard PJ, Mao F, Leung W-Y, Haugland RP: **Alexa Dyes, a Series of New Fluorescent Dyes that Yield Exceptionally Bright, Photostable Conjugates**. *J. Histochem. Cytochem.* 1999, **47**:1179-1188.
99. Tsurui H, Nishimura H, Hattori S, Hirose S, Okumura K, Shirai T: **Seven-color fluorescence imaging of tissue samples based on fourier spectroscopy and singular value decomposition**. *J. Histochem. Cytochem.* 2000, **48**:653-662.
100. Turner L, Ryu WS, Berg HC: **Real-time imaging of fluorescent flagellar filaments**. *J. Bacteriol.* 2000, **182**:2793-2801.
101. Horne JH, Meyer T: **Characterization of a dextran-based bifunctional calcium indicator immobilized in cells by the enzymatic addition of isoprenoid lipids**. *Cell Calcium* 1999, **25**:1-7.